Lumped Parameter Modeling of Hybrid Electromechanical Valve Actuator

Saad Ali
00000171403

Supervisor
Dr. Jawad Aslam

DEPARTMENT OF DESIGN AND MANUFACTURING ENGINEERING
SCHOOL OF MECHANICAL & MANUFACTURING ENGINEERING
NATIONAL UNIVERSITY OF SCIENCES AND TECHNOLOGY
ISLAMABAD, PAKISTAN
AUGUST 2018

Lumped Parameter Modeling of Hybrid Electromechanical Valve Actuator

Author

Saad Ali

Registration Number

00000172533

A thesis submitted in partial fulfillment of the requirements for the degree of

MS Design and Manufacturing Engineering

Thesis Supervisor:

Dr. Jawad Aslam

Thesis Supervisor's Signature: _____

DEPARTMENT OF DESIGN AND MANUFACTURING ENGINEERING

SCHOOL OF MECHANICAL & MANUFACTURING ENGINEERING

NATIONAL UNIVERSITY OF SCIENCES AND TECHNOLOGY

H-12 ISLAMABAD, PAKISTAN

AUGUST 2018

Thesis Acceptance Certificate

Certified that final copy of MS/MPhil Thesis Written by **Saad Ali** (Registration No: **00000171403**), of SMME (School of Mechanical and Manufacturing Engineering) has been vetted by undersigned, found complete is all respects as per NUST Statutes/ Regulations, is free of plagiarism, errors and mistakes and is accepted as partial fulfillment for award of MS/MPhil Degree. It is further certified that necessary amendments as pointed out by GEC members have also been incorporated in this dissertation.

Signature: _____

Name of the supervisor: Dr. Jawad Aslam

Date: _____

Signature (HOD): _____

Date: _____

Signature (Principle): _____

Date: _____

FORM TH-4

National University of Science and Technology

MASTER THESIS WORK

We hereby recommended that the dissertation prepared under our supervision by **Saad Ali** (00000171403) titled: "**Investigation into the machinability of non-conventional alloys (Inconel 718)**" be accepted in partial fulfillment of the requirements for the MS Design and Manufacturing Degree with (___) grade.

Examination Committee Members

1. Name: Dr. Samiur Rehman Shah Signature: _____

2. Name: Dr. Mian Ashfaq Ali Signature: _____

3. Name: Dr. Hussain Imran Signature: _____

Supervisor Name: Dr. Jawad Aslam Signature: _____

Date: _____

_____

Head of Department Date: _____

COUNTERSIGNED

Date: _____

_____

Dean/Principal

Declaration

I certify that this research work titled **"Lumped Parameter Modeling of Hybrid Electromechanical Valve Actuator"** is my own work. The work has not been presented elsewhere for assessment. The material that has been used from other sources it has been properly acknowledged / referred.

_____

Saad Ali

00000171403

Plagiarism Certificate (Turnitin Report)

This thesis has been checked for Plagiarism. Turnitin report endorsed by Supervisor is attached.

_____

Saad Ali

00000171403

Dr. Jawad Aslam

Signature: _____

Copyright Statement

Acknowledgements

I am thankful to my Creator Allah Subhana-Watala to have guided me throughout this work at every step and for every new thought which you setup in my mind to improve it. Indeed, I could have done nothing without your priceless help and guidance. Whosoever helped me throughout the course of my thesis, whether my parents or any other individual was your will, so indeed none be worthy of praise but you.

I am profusely thankful to my beloved parents who raised me when I was not capable of walking and continued to support me throughout in every department of my life.

I would like to express special thanks to my supervisor Dr. Jawad Aslam for his guidance and help throughout my research work.

I would also like to pay special thanks to Muhammad Nauman Rafique from USPCAS-E, NUST for his tremendous support and cooperation. Each time I got stuck in something, he came up with the solution. Without his help, I wouldn't have been able to complete my thesis.

I would also like to thank my co-supervisor Dr. Mushtaq Khan and members of evaluation committee Dr. Samiur Rehman Shah, Dr. Mian Ashfaq Ali and Dr. Hussain Imran for their valuable advice. I am also thankful to Mohsin Ali, Muhammad Athar Ali, Nabeel Mushtaq and Ahmad Faraz for their support and cooperation.

Finally, I would like to express my gratitude to all the individuals who have rendered valuable assistance to my study.

Dedicated to my exceptional parents and adored siblings whose tremendous support and cooperation led me to this wonderful accomplishment?

Abstract

Automobile engine Valve actuation is of primary importance in the field of internal combustion engines. The conventional engine uses camshaft for valve operation which can be varied to a certain extent with the engine speed variation. The variable valve timing is an alternative to the conventional camshaft operated engines with the improved valve timing variation. The variable valve timing technology developed cannot provide continuous valve timing variation and resulted in improvement in valve timing variation to a limited scope. The effective alternative to the camshaft engines is camless valve actuation system with the advantage of fully flexible valve timing according to the engine speed variation leading to fuel efficient engine operation. The camless valve actuation systems include electromechanical, hydraulic, piezoelectric, pneumatic and hybrid actuators with combination of actuators. A modified hybrid valve actuator (MHVA) with combined effect of electromagnet and permanent magnet was designed and validated using FEM and prototype testing. A lumped parameter model (LPM) was developed to approximate the experimental and FEM results of MHVA using valid mathematical expressions. The LPM is developed based on the physical parameters identified by curve fitting of experimental force data and mathematical equations representing the coil dynamics, force and armature dynamics of MHVA. The electrical, magnetic and mechanical subsystems are developed in MATLAB and integrated to develop LPM. The results of LPM are compared with the experimental and FEM results to validate the lumped parameter model developed in this study.

Key Words: *Electromechanical valve actuator (EMVA), Lumped parameter model (LPM), Modified hybrid valve actuator (MHVA), Finite element method (FEM), Camless engine*.

Contents

List of Figures

CHAPTER 1: INTRODUCTION

1.1 Introduction

To achieve optimal fuel efficiency and reduced emissions, valve timing must vary as engine rotational speed varies. The conventional method of operating valve train in the internal combustion engine is through the use of camshafts. The limitation of this system is having fixed values for valve lift, event timing and durations. This leads to a compromise between different requirements for continuously varying operating conditions. These conventional engines have fixed valve events that can be optimized to only a fraction at engine development stage to meet certain engine load and speed requirements. The design of camshaft lobe profile requires a compromise between maximum fuel efficiency and high torque performance. Reasonable research has been done for designing and developing camshaft based variable valve timing mechanisms but the problem was solved to only a small fraction. Variable camshaft timing mechanisms were implemented and analyzed by F. Bonatesta *et al.* [1], on two small sized spark ignition engines. The mechanisms were tested and the results showed average values of fuel consumption reduction of 3.5% on all part-load conditions. Optimization, fully flexible timing and valve lift is not possible with the camshaft based engines.

Variable engine valve timing mechanism can provide a practical substitute to the conventional camshaft engine valve system. This technique has the advantage of controlling the valve events without the dependence of crankshaft rotation. Full flexible timing and valve lift can be achieved using this mechanism. Different types of actuators were used by the researchers to achieve flexible variable timing including mechanical, hydraulic, motor driven and electromagnetic actuators.

Amongst different actuator technologies used by the researchers at experimental level, the electromagnetic actuator has proved to achieve more promising results by improving the engine performance and reducing the emissions. The actuator is composed of a solenoid which can be electronically controlled. Its construction is very simple and low cost, making the engine less complex and light weight. These light weight and cost-effective actuators must be designed to withstand cyclic loads during the engine operation. In spite of the benefits of electromagnetic

and other actuators, the practical application of such devices on commercial automobile engines is quite challenging. The problem requiring most attention is lowering of the impact velocity at the end of valve seating position. This problem will cause noisy engine operation and wear issues in the later stages of engine life. This conundrum is largely due to the actuator's nonlinearity in the behavior of magnetic actuator and its sensitivity to disturbances and parameter uncertainties. In order to implement the EMV actuators in commercial automobile engines, robust control method must be designed and developed to achieve reasonably lower velocities at the seating position of valve [2].

This work is focused on development of mathematical model of already designed hybrid valve actuator prototype and its experimentation on test bed. The prototype actuator is a novel hybrid mechanism comprising of axis-symmetric permanent magnet and electromagnet magnetomotive force actuator. This prototype has the benefits of achieving large values of magnetic force consuming very low energy, low value of coil inductance, permanent magnet demagnetization isolation, and improved transient response. The mathematical modeling is done for experimental determined magnetomotive force varying with armature position. The current transient response with time is also modeled and finally a lumped parameter model is developed representing the performance of hybrid actuator prototype. The lumped parameter model is compared with the experimental and simulated FEA model. On the basis of lumped parameter model, an adaptive control design can be developed to improve the performance of hybrid actuator prototype and to achieve desired design requirements of lowered impact velocities and relatively smoother velocity profile of actuator with continuously varying engine load and speed.

CHAPTER 2: LITRATURE REVIEW

2.1 Introduction

VVT technologies based on various actuators have been implemented on laboratory scale by many researchers and the technology has proved to be potentially beneficial by improving engine performance parameters. The idea of independent valvetrain with electrically controlled valve gears was patented by Payne D. in 1899. The variable timing achieved in the VVT devices is far better than cam based engine improvements [3]. The implementation of VVT devices in automobile engines on commercial scale is still far from reality due to the need of essential design improvements not addressed by the researchers. The achievement of robust control of seating valve velocity is on of most important design requirement for error free long term application of VVT in commercial automobile engines. Only Swedish automobile manufacturer Koenigsegg and Chinese automobile manufacturer Qoros have developed prototype automobile based on VVT devices.

2.2 Motor driven actuator

Engine testing was conducted using an experimental setup based on one cylinder of a modified engine with specifications of six cylinder 3.8-liter, with an innovative motor driven mechanisms for valve operation [4]. Experimental tests showed variable valve timing with low fluctuations in profiles of valve lift with additional control of valve seating velocity and noise.

2.3 Electrohydraulic Actuators

Fully flexible electro-hydraulic valve actuator was developed and tested in laboratory. Based on the experimental results, a dynamic mathematical model was developed and used in control design and implementation using dSpace system [5]. Valve profile tracking errors were achieved in the range of 140 microns for a 9.5 mm valve lift at engine speed of about 3000 rpm.

Transient control of fully flexible electro-hydraulic actuator is implemented to provide accurate valve profile tracking under both conditions of constant and varying engine speed [6]. The time-varying periodic profile tracking problem was converted into a periodic profile and a constant profile having time-varying duration. Repetitive control was implemented to track the periodic profile and PID regulator to track the constant profile. The control method was

successfully implemented on an electro-hydraulic actuator having transient capabilities including lift transient, duration transient, phasing transient, speed transient, and mode transient.

An indirect adaptive backstepping controller was developed for an experimental electrohydraulic test bench [7]. Electrohydraulic systems are difficult to model as they are highly nonlinear and nondifferentiable. Indirect adaptive control is highly recommended, among other adaptive controller types, as it has the benefit of identifying the real system parameters value. The results of control development were compared with a real-time non-adaptive backstepping controller and with the results from similar works in literature. It was concluded from the results that indirect adaptive backstepping control technique is the ideal for using in hydraulic systems control as provides the real physical values of the system parameters for system monitoring.

Reduced-order nonlinear and linear parameter-varying models were presented for an electro-hydraulic variable valve actuation system by H. Li *et al* [8]. The modeling included nonlinear mathematical system model developed using the Newton's law, orifice flow equation, and fluid constitutive law. For the development of linear parameter-varying model, the order of nonlinear model was reduced and consequently transformed into an LPV model having reduced deviation by incorporating the system nonlinearities, time delay, and time-varying. Both the developed models including the reduced-order nonlinear and LPV provide the basis for development of control strategies for the electric-hydraulic variable valve actuation system.

An innovative electromechanical variable valve system is introduced by P. Wong and K. Mok [9]. The design was based on a cam operated mechanism and its integration was done into an electrohydraulic system. The electrohydraulic system was designed to provide input hydraulic pulses which were used to drive the intake and exhaust valves. The operating valve profile was electronically controlled by a pressure relief valve. The mathematical modeling of the variable valve system along with its dynamic analysis was presented in this study.

One way of varying valve timing according to requirements is through an electro-hydraulic valve system. The study by H. H. Liao *et al* [10], first describes an identification method for obtaining a mathematical model of the EHVS. Based on the mathematical modeling, a linear feedback controller is designed and developed. A repetitive feed-forward controller is then used along with linear feedback controller to amplify the feedback controller.

2.4 Electropneumatic actuators

A comprehensive dynamic model of camless actuator based on electropneumatic valve actuation technique for engine gas valves was developed by J. Ma *et al.* [11]. The experimental setup of proposed model has two actuation systems, one is the pneumatic actuation and the other is hydraulic latch mechanism. The purpose of the pneumatic actuator is to open the valve and the hydraulic latch system performs two functions, to keep the valve open and to reduce valve seating velocity. The mathematical modeling of air and liquid compressibility in the hydraulic latch was done considering discontinuous nonlinearity of the compressible flow due to choking. The model was verified by experiments performed on a Ford 4.6 l four-valve V8 engine head by varying operating conditions of air pressures and solenoid pulse inputs. The experimental results were in agreement with modeled responses.

An adaptive valve lift control strategy based on mathematical nonlinear system model was developed to improve the valve lift repeatability[12]. The closed-loop valve lift control strategies in combination with the model reference feedforward control were developed and implemented in a prototype controller. The results of controller were validated on a test bench for valve with multiple reference valve lifts at 1200 and 5000 r/min engine speeds. The comparison of results indicated that lift error was within the range of 0.5mm in one cycle at 1200 r/min and in two cycles at 5000 r/min. The maximum steady-state lift errors at both high and low valve lift were less than 0.4mm and less than 1.3mm respectively. The closed-loop valve lift control showed enhanced valve lift repeatability that is more than 30% reduction of standard deviation in comparison with open-loop control.

Based on the mathematical model of pneumatic valve actuation system, a control design was developed by T. Nguyen *et al.* [13] for a sliding pneumatic motion control system using four solenoid valves with a position feedback sensor. The results of simulation and experiments were in agreement depicting robustness of model and control system with considerably low steady-state position errors.

2.5 Piezoelectric valve actuators

Design of an actuator mechanism using piezoelectric ceramic ‘PZT’ was done by N. Jalili *et al* [14], with a desired feature of stepping motion amplifier to provide desired force and displacement at varying loading conditions with the advantages of lightweight, high frequency,

precise position solution for continuously varying valve timings. Experimental results demonstrated the feasibility of the system consisting of piezoelectric ceramic 'PZT' based camless valvetrain. The system of valvetrain exhibited desired cam-based performance parameters with opportunity of computer based control of individual valve timing parameter.

Most of proposed piezoelectric based actuators are hybrid actuators combining the piezoelectric actuator with hydraulic or electromagnetic actuators for lowering energy consumption and enhanced operating characteristics. A nonlinear mathematical model of hydraulic actuation system was proposed, regulated by novel hybrid piezo-hydraulic valve spool presented by a linear model [15]. A nonlinear control strategy was proposed and implemented utilizing a combined feedforward and feedback control. A decoupling feedforward control was implemented for the required positioning of the valve spool and a sliding mode control was proposed to track desired trajectories of engine valve the engine valve. Performance and the effectiveness of the proposed control strategy were demonstrated by results of simulations.

2.6 Electromagnetic actuators

A finite-element analysis model was developed by R. Chladny *et al* [16] to describe time dependent and time independent operation of intake and exhaust valves. Solenoids were used to control these valves and application of such valves resulted in improved engine efficiency. Results of testing performed in laboratory validated the benefits of using solenoid actuated valves. A nonlinear lumped-parameter model using the FEA results was also developed in comparison with experimental results.

Electromagnetic actuator to drive valvetrain was designed, modeled and analyzed by C. Niţu *et al* [17],with required dynamic performances for varying load conditions and the system was experimentally tested in laboratory using electronic controller and corresponding software. The replacement of feed-forward controller with an energy based feedback controller solved the problems faced due to varying combustion forces

An indirect valve position measuring method was developed by F. Ronchi *et al.* [18], for camless electromagnetic actuator system. The position measuring method used flux signals obtained through integration of a secondary coil voltage at each electromagnet. This method provides both fluxes and position signals utilized in the designing of feedback position

controller. The paper [18], described about accuracy obtained for position reconstruction and linked it to the system parameters tolerances. Experimental results validated the proposed solution.

An electromechanical valve drive system was custom-designed with limited-angle actuator by Y. Qiu *et al.* [19], that was feasible with limited power consumption smaller package, and quicker transition was predicted by simulation.

Variable valve timing was achieved using a mechanism based on planetary gears by K. Nagaya *et al.* [20]. The outer gear served the purpose of timing pulley having a timing belt getting power from crankshaft of an engine. Disc center having the centers of the planetary gear is engaged to the camshaft. The system provided the continuous control of valve phase and lift Finite element modeling and design of high-speed solenoid actuators was developed by S. Khan *et al* [21], having operating frequencies ranging from 150-300 Hz with advantage of large force 8-15 N produced by the actuators and long lifetime of 2-5 billion cycles offered by them.

The paper [22] focused on the valve seating velocity and holding force with moving coil linear actuator. The electromagnetic valvetrain system developed by L. Liu and S. Chang [22], had benefits of achieving low valve seating velocity. Two parameters described the performance and efficiency of the system including seating velocity and holding force. The valve was controlled to track required trajectory which was based on inverse system method to lower valve seating velocity. PID current controller was used to control the holding force to get the surety of sealing of cylinder. An experimental testing setup validated the concept. Seating velocity of the valve actuator was minimized by designing a tracking controller consisting of linear feedback and non-square iterative learning controller.

A lumped parameter model of electromechanical valve actuator was developed by A. di Gaeta *et al*. [23], based on a hybrid analytical–finite-element method (FEM) approach. The mathematical model was developed to apply sensorless approach of reducing impact velocity of valve. A mathematical function was used to quantify global magnetic parameters as the flux linkage and force for the cases of linear and non-linear saturation regions. The response of dynamic behavior of the model was then tested on transient FEM simulations of the actuator under various working conditions. A dynamic LPM was developed to describe magnetic

behavior of the actuator. Nonlinearities including self or mutual inductances and back EMF were also taken into account in the model. The dynamic response of the LPM was in agreement with FEM data attained by simulating the magnetodynamic DPM of the actuator under different conditions for a fixed and moving valve. LPM developed provided the foundation for implementing the control strategies for controlling impact velocities during valve operation.

A multiobjective optimization of electromagnetic valve actuator and energy compensation control strategy was developed by Y.-P. Yang, *et al*. [24]. This axisymmetric and cylindrical actuator incorporated a hybrid magnetomotive force with both the permanent magnet and electromagnet. The dynamic model of the electromagnetic actuator was developed in accordance with a magnetic circuit providing the basis for optimal design function used for satisfaction of multiple objectives including magnetic holding force, release current and its rising time. Sensitivity analysis was performed using the dynamic model. The energy compensation strategy was successfully applied to implement the soft valve landing control of proposed EMVA which comprises a cylindrical actuator, a permanent, an electromagnet, and a secondary air gap for prevention of irreversibly demagnetizing. The simulation and experimental setup comprising a four-stroke, spark-ignition engine, showed reduction of landing velocity of the valve to a few milliseconds and the power with the implementation of compensation control.

An electromagnetic valve actuator comprising a permanent magnet was simulated in matlab and Maxwell by S. H. Lee *et al*. [25]. The objective of research was to reduce the transition time of the electromagnetic valve by maximizing the vibration frequency of the armature. The actuator performance was optimized based on genetic algorithm, 2-D and3-D finite element analysis resulting in increase of vibration frequency by 30. The transition time of stroke was reduced by 8.7%, enhanced maximum engine speed as compared to conventional electromagnetic actuators.

A position observer and a velocity estimator was proposed by P. Mercorelli *et al.* [26] for observing the position and velocity of an electromagnetic valve actuator in a sensorless manner. Both the observer and estimator were combined in a cascade structure. Lyapunov nonlinear approach was used to design position observer and modeling of a proposed valve actuator was used to design velocity estimator. The coil current is the input signal for observing the position in the position observer based on Lyapunov nonlinear approach and the valve velocity is the output

signal. The position and velocity values obtained were compared with those of extended Kalman filter used as reference. A control strategy based on discrete and analogous proportional derivative (PD) controller was implemented in combination with a feedforward action compensating the stationer error.

The problem of high power consumption in operation of electromagnetic actuators valve actuators was targeted and a solution was proposed by A. Fabbrini *et al.* [27]. Based on the physical properties of the system and local flatness, a constrained optimization was performed. An industrial simulator of the valve actuator was used to validate the design trajectory performance. The trajectory design was used in the control implementation for the position control actuator and ultimately the control of the impact velocity of valve. The main difficulty is represented by structural physical constraints of the actuator. A technique was proposed to minimize the power consumption by considering the structural constraints. The results of simulations showed reduction of the power consumption utilizing brute force optimization in the trajectory space.

In a study by J. Tsai *et al.* [28], the valve control methodology was categorized into landing controllers, controlling the 8mm valve displacement and the remaining displacement by approach controllers**.** The focus of the research was to implement approach control controlling the initial conditions which ultimately helped in controlling the landing**.** Simulations based on three different cyclic adaptive feedforward approach controllers including nonlinear iterative learning, terminal iterative learning, and Nelder Mead direct search algorithms were performed**.** The simulated and experimental results of the three approaches were compared and the results showed that Nelder Mead approach performed better than other approaches. The results of simulation and experiment showed that after 100 to 150 valve operating cycles, the Nelder Mead controller rejected the effect due to step disturbance force of 40 N. It was concluded that Nelder Mead controller performed satisfactorily regarding optimization capability, robustness against disturbances, and computational efficiency for approach control of electromagnetic actuator.

A control design based on voltage constraints, nonlinear magnetic effects, and valve motion requirement was proposed and tested by Soon K. Chung *et al*. [29]. Design parameter was a flat output, parameterized on spline basis. A linear stable tracking error system was obtained utilizing the flat output providing feedback open-loop control. The experimental and simulated

results were in agreement with each other. The flatness-based method was compared to PI controller experimentally. The control algorithm was implemented based on the lumped parameter modeling of electromagnetic valve properties including the nonlinear effects of magnetic saturation and eddy current. The flatness based control implementation resulted in consistent low impact velocity of valve and the PI control produced high magnitude, varying velocity.

The simulations based on finite element method (FEM) was performed by [30], to produce static force and flux data and the results of simulation were validated by experimental testing. An ordinary differential equation model was utilized to implement a non-linear flatness-based estimated state feedback control. The force and flux data obtained from FEM model was used to develop the lumped parameter model and the results of simulations performed on Simulink showed low impact velocities.

A possible number of table-based lumped-parameter models of linear or rotary actuators were compared [31]. Among these LP models, two of the models were computed in this study which was not published in previous studies. The results of simulation and experimentation for all the considered models of actuators were compared. The models presented in the study assumed one-coil devices, but the methodologies were applicable to multicoil.

2.7 Hybrid actuators

Design calculation and model of direct drive electromagnetic valve actuator was presented by D. Cope *et al* [32]. The actuator was capable of flexible valve timing and valve lift with the advantages of higher engine efficiency, reduction in emissions, and better control of end performance. The designed actuator composed of stationary permanent magnets, stationary coils, and a moveable plunger made of steel which was used to transmit required bi-directional forces to the valve. Variable valve timing offers advantages for improving the fuel economy and emissions of internal combustion engines

An innovative hybrid electromagnetic actuators consisting of both permanent magnet and electromagnetic coils was designed by Y. Shiao and L. V. Dat [33], to overcome the drawbacks of existing electromagnetic actuators. This hybrid electromagnetic actuator consisted of a simplified physical structure, simplified actuation with very low power requirement for

actuation. Magnetic simulation was done to get the analysis of the magnetic flux density of the electromagnetic valvetrain and to achieve optimization of the design parameters. Using a permanent magnet with an optimized actuating current to catch and release valves is beneficial in energy consumption in comparison with existing electromagnetic valvetrains.

Intake and exhaust valves with fixed timing events irrespective of engine speed leads to a compromise between fuel consumption exhaust emissions and torque. Various automobile companies have designed and tested solenoid intake and exhaust valve actuators to achieve variable valve timing. The designed valvetrains were consuming higher power making them not feasible for use in engines of commercial automobiles. The study by J. Kim and D. K. Lieu [34], introduced a novel electromagnetic valve actuator that used permanent magnets to control the valve position reducing the consumption of power.

A mechanism based on four-corner suspension model having a piezoelectric piloted hydraulic actuator was tested by J. S. Brade *et al* [35], for engine valvetrain control. Control problems were addressed using the relationship between input voltage and piezoelectric displacement by the implementation of piezoelectric based camless engine actuator.

A hybrid actuator based on a piezoelectric and a hydraulic part having a switching Kalman Filter structure was proposed by P. Mercorelli *et al.* [36]**.**. Preisach dynamic model having a robust switching Kalman Filter was used to take into account the nonlinear behavior of hysteresis. A Model predictive control was utilized to realize the control structure and the results of simulations were also presented in the study. The position and velocity of a valve were controlled using the predictive control strategy by utilizing the input current and voltage.

A linear reluctance motor actuator comprising a permanent-magnet technology proposed in the study and it is intended to be used as an electromagnetic engine valve drive. A velocity switching estimator was proposed by P. Mercorelli *et al.* [37]**,** using the current and input voltage data to achieve sensorless control of actuator. A minimum variance approach was utilized in determining the robustness of velocity control. The control of valve position can be achieved by inversion of model utilizing an adaptive and optimized structure, comprising of a velocity estimator and an observer for the electromechanical system. The results of simulations are

presented showing effectiveness of the observer with optimization of parameters in the closed-loop control.

A hybrid actuator comprising of a piezo for its high precision and a hydraulic part to obtain force required for movement of valve in the actuator was proposed by P. Mercorelli *et al*. [38]. A control strategy based on cascade PI-PID-PI control structure was presented. Preisach dynamic model of the piezoelectric actuator was considered taking into account the nonlinearities related to it. A control design based on a model having a switching function was also implemented.

An electromagnetic actuator based on the hybrid magneto-motive force implementation was proposed by J.-J. Liu *et al.* [39], in which the magnetic flux was obtained by the coil excitation and permanent magnets. Design of a dual flux channels EMVA was presented in the study. The current requirement at the start of operation was reduced due to close position of valve due to holding force of permanent magnet at the time of no current supplied into the coil. The permanent magnet helped in lowering the power requirement for the proposed actuator.

A hybrid piezoelectric actuator was presented by P. Mercorelli *et al.* [40], comprising a piezoelectric, a stroke ratio displacement, a mechanical and a hydraulic part. The study focused on design issues of actuator related nonlinear hysteresis effect, scaling force position to achieve required displacement of the actuator and control implementation of hybrid system. A cascade feedforward control strategy was proposed based on model of actuator, in combination with an internal and an external PI-Controller. Hydraulic pressure faults were compensated by adaptive feedforward action of controller. Adaptive Feedforward Control composed of two Euler inversions as Feedforward Controllers and a simple PI as a Feedback Controller.

Due to a lack of bandwidth separation, it is unclear which combination of feedback signals would be most advantageous for controlling electromechanical valve actuators. To address this issue, this paper investigates the use of position, current, and flux measurements in the feedback. Based on the analysis, a combination of position and flux best achieves the design specifications without incurring large control signals.

A modified hybrid valve actuator (MHVA) was designed, validated by J. Aslam *et al* [41], using FEM in Ansys Maxwell and experimentation on test bed. The MHVA design include permanent magnet in addition to electromagnet and parallel solenoid coils for controlling PM

and EM reluctance. The addition of permanent magnet assisted in latching the armature at the valve seating position and leads to reduction of power consumption by the MHVA system. The research work in this thesis comprises of lumped parameter model (LPM) development using S-function in Simulink module of MATLAB on the basis of experimental results performed by previous study and mathematical equations representing important physical quantities. The mathematical model can be used in the development of control strategies and can be tested on experimental test bed.

2.8 Summary

Camless valve actuation systems are of primary concern for the researchers in the curiosity to reduce the fuel consumption and exhaust emissions to reduce cost and environment friendly automobile engine operation. The conventional camshaft can be replaced using one of the valve actuation system developed and tested by the researchers. The valve actuation systems which are of interest for the researchers include electromechanical valve actuator, hydraulic actuator, pneumatic actuator, piezoelectric actuator, motor operated actuator, planetary gear based actuator and hybrid actuators taking the advantage of properties of more than one actuator technology. Electromagnetic actuator has been tested in combination with the permanent magnet which reduces the energy consumption making the actuator energy efficient. In this study, the electromagnetic actuator with combination of permanent magnet is modeled using experimental and FEM results of MHVA previously studied and mathematical expressions representing physical quantities including coil current, force for driving the armature and armature displacement and velocity.

CHAPTER 3: BRIEF DESCRIPTION OF ANSYS SIMULATION AND EXPERIMENTATION

3.1 Introduction

The design of modified hybrid actuator is discussed in this chapter in detail. The design involves brief theoretical explanation of important magnetic parameters including flux, flux density and magnetic field strength and their dependence on geometrical features of coils including area of coil and core. The basic components of hybrid actuator are discussed in this chapter. The analysis of design using FEM technique is also included. The brief description of fabrication, assembly and testing performed by J. Aslam *et al* [41] is included. Based on the FEM and experimental results obtained from the previous work, a lumped parameter model is developed and the results are compared with already performed FEM analysis and experimentation.

3.2 Design Theory of MHVA

The physical structure of hybrid actuator consisted of stationary permanent magnet and coils with reciprocating armature. The geometrical features of actuator included bi-directional, axis symmetry, modified cylindrical core with properties of I-core for holding force and cylindrical core for force at equilibrium position and inverse coil current. The design of actuator estimated the generation of approximately 200N holding force at equilibrium position in presence of coil current and 500N force at the armature seating position in absence of coil current. The higher magnitude of force required at the seating position was to overcome higher exhaust gas pressure during operation of engine cycle and spring force.

$$\varphi = B \times A_{core} \tag{3.1}$$

$$A_{core} = 2\pi rl + 2\pi r^2 \tag{3.2}$$

$$H = \frac{B}{\mu_o} \tag{3.3}$$

$$I = \frac{Aturn}{N} \tag{3.4}$$

$$F_H = \frac{B^2 A_{pole}}{2\mu_o} \tag{3.5}$$

Here the values of A_{pole}, B and μ_o for the proposed design of hybrid actuator are $2.5 \times 10^{-4}\text{m}^2$, 2.74587Wbm^{-2} and $4\boldsymbol{\pi} \times 10^{-7}\text{TmA}^{-1}$. The value of A_{pole} is the overall area of three poles of cylindrical core. The overall flux can be calculated using the mathematical relation given in Eq. (3.6).

$$\phi = BA_{core} \tag{3.6}$$

Here the value of surface area of core is $1.095 \times 10^{-4}\text{m}^2$. The value of flux comes out to be $30.067 \times 10^{-5}\text{Wb}$. The magnetic field strength can be calculated by dividing the flux density with permeability of free space and it was calculated to be 2185093.91 ATm^{-1}.The magnetomotive force was obtained by multiplying air gap with the field strength and it was calculated to be 8740.37 Aturns for 4mm air gap.

The components of hybrid actuator consisted of two springs in pre-compression state for positioning of armature at equilibrium state between two solenoids. The soft iron yoke was further divided into three components including yoke, yoke cover plate and yoke base plate with secondary air gaps between them. The purpose of air gaps was to prevent flux circulation through permanent magnet leading to demagnetization. The flux of both permanent magnet and electromagnet are directed in parallel direction to each other. The reluctance of permanent magnet provided holding force for latching armature at seating position without interference of electromagnet. The application of two similar cylindrical coils having same number of turns and wire diameter directed parallel to each other helped in reducing overall inductance and resistance, leading to rapid current rise. Flexible independent coil control guarantees low energy consumption. The soft iron former house PM and provide structure for armature seating. The soft iron former provided seating of armature and harmonic stresses due to armature oscillations were absorbed by the iron former. The brass bush used in the assembly separated the iron former and armature stem and alignment of armature stem. The schematic diagram of modified hybrid actuator with each component labeled is shown in Fig. 1, describing the basic configuration of proposed hybrid valve actuator design. The proposed design was verified using Ansys simulations, experimentation and lumped parameter model based on the experimental results.

The results obtained using the three different procedures including Ansys simulations; experimentation and mathematical modeling were compared to validate the proposed actuator design.

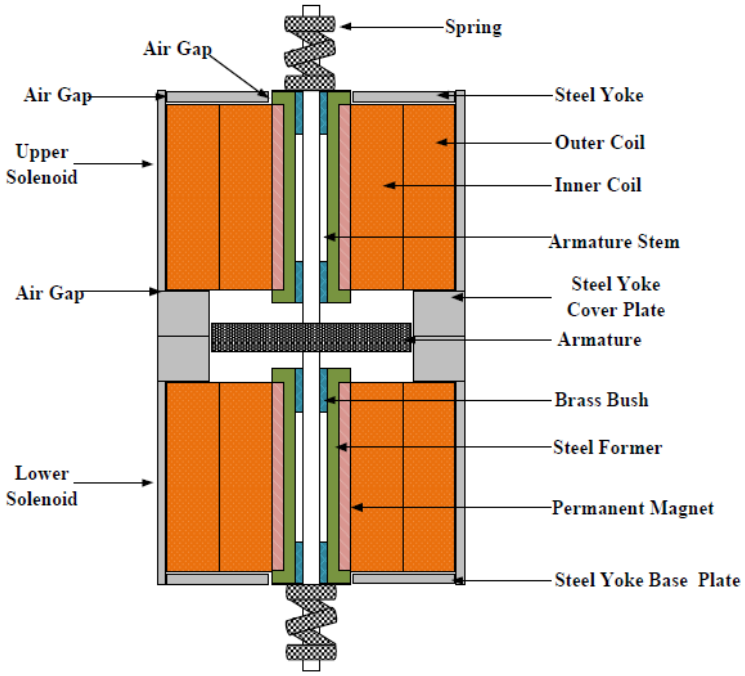

Figure 1 Schematic diagram of MHVA

3.3 Finite Element Analysis of MHVA

The FEA technique was applied using Ansys Maxwell software for parametric analysis of designed hybrid actuator by developing equivalent hybrid actuator in the software. The armature holding force was analyzed by varying the parameters of construction. The holding force was found to be dependent upon physical parameters including dimensions of assembly components which are armature, yoke, yoke cover plate, yoke base plate, PM and air gaps. The model was divided into finite elements nodes for the purpose of analysis based on the magnetic vector potential, boundary conditions and initial conditions of individual node. Electromagnetic force and field distribution for each node was calculated using Maxwell equations. The Ampere Law is given by the Eq. (3.7).

$$\nabla \times H = J \tag{3.7}$$

In the above equation, H is magnetic field strength; J is the current density and is the curl operator. The Gauss law can be written mathematically as shown in Eq. (3.8).

$$\nabla \times B = 0 \tag{3.8}$$

The magnetic field B and magnetic field strength are related in the Eq. (3.9), where μ_r denoted the relative permeability.

$$B = \mu_r \mu_o H \tag{3.9}$$

Combining Eq. (3.7) and Eq. (3.9), we can get the relation shown in Eq. (3.10).

$$\nabla \frac{B}{\mu_r \mu_o} = J \tag{3.10}$$

The force can be represented mathematically by Eq. (3.11), where 'I' is the coil current and dl is the vector length.

$$F = \int Idl \times B \tag{3.11}$$

In the analysis performed on ANSYS Maxwell, uniform magnetic field was assumed in the circumferential direction due to axis symmetrical geometry and thus the current density is also uniformly distributed. The magnetic field generated by permanent magnet is constant and the magnetic field generated by electromagnet is also constant if current is kept constant and in this way the current can be treated as static field. A 2D static analysis was performed using initial parameter values in ANSYS Maxwell for optimal MHVA design. The effects of parameter were studied by variation in geometry of actuator. The valve lift span for the FEA methodology was the same as considered in previous design. Both the solenoids were modeled separately due to axis symmetry reducing the modeling complexity and computational time.

The geometric parameters of armature with assigned material of steel-1008 included in the analysis are Armature width and thickness. The analysis showed the effect of holding force to varying armature width and thickness indicating 73.75% enhancement of holding force with 7mm increment in armature width and 45.43% increase with 3mm increment of armature thickness. Spring of higher spring constant and larger sized permanent magnet must be required with increasing the armature dimensions. It was observed from the analysis that for the design

requirement of 500N holding force the optimal armature dimension values of width and thickness were 22mm and 5mm.

The effects of height and thickness of permanent magnet with assigned material of NdFe35 indicated rise of 96.29 % in holding force with increase of 40mm in height and 61.36% rise in holding force with 4mm rise of thickness of permanent magnet. The dimensions of permanent magnet were observed to be directly proportional with inverse current required for reduction of permanent magnet reluctance and energy consumption. The optimal values permanent magnet dimensions were 50mm and 4mm for 500N holding force and low inductance requirement.

The air gap of yoke and yoke base plat from the former lead to enhancement of holding force required for catching the armature at the time of coil excitation and reduction of holding force for release of armature on inverse coil current application. The holding force was observed to be less sensitive to yoke dimensions including yoke height and width, base plate thickness and width. The increment of 13.5mm, 4mm, 12mm and 3mm in the yoke height and width, base plate thickness and width showed increment of 9.52%, 0.51%, 8.82% and 2.45 % in holding force. The optimal yoke dimensional values including height and width of yoke, width and thickness of yoke base plate were observed to be 55.5mm, 3mm27mm and 5mm respectively to fulfill the requirement of 500N holding force. Increasing the yoke cover plate dimensional parameters resulted in the increment of flux concentration area of armature leading to rise of holding force. With the rise of 8.5mm in width and 7mm in thickness of yoke cover plate resulted in 52.29% increase and 21.52% increase in holding force respectively. The optimal values of yoke cover plate dimensional parameters including width and thickness were observed to be 17.5mm and 9 mm respectively.

Air gaps Ga1 lead to the detouring of flux and isolated the permanent magnet from demagnetization. Increment in the air gap Ga1 indicated 66.3% rise in the holding force and increasing the air gaps Ga2, Ga3 and Ga4 indicated decrement in holding force by 4.88%, 12.55% and3.04% respectively. The optimal values of air gaps were observed to be Ga1=1 mm, Ga2=0.2 mm, Ga3=0.5 mm and Ga4=0 mm.

The static FEM analysis was performed using three ampere-turn values of 500, 1000 and 1500 excitation currents and at zero ampere-turn representing the force due to permanent magnet. The optimal dimensional parameters obtained previously were utilized in modeling of

modified hybrid valve actuator. The static analysis was performed to show the effect of air gap on magnitude of electromagnetic force. The force variation with respect to air gap for three different magnetomotive force values of 500, 1000 and 1500 Aturns and at 0 Aturn is plotted in the Fig. 2.

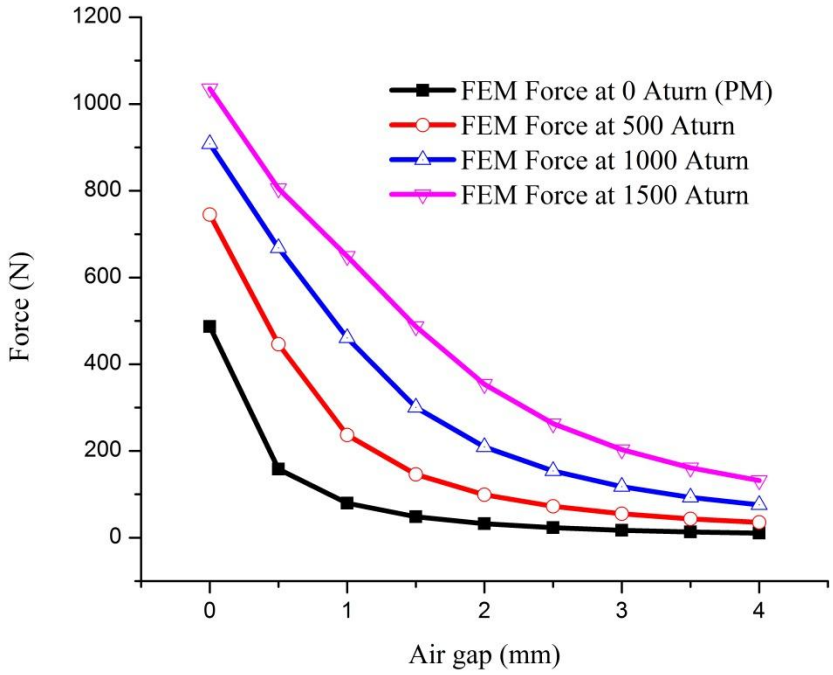

Figure 2 FEM Analysis of magnetomotive force response (PM and EM)

The contour lines were plotted closer to armature for the analysis of flux leakage and fringing effect. The lines predicted the flux density and steady or unsteady nature of flux. The highest flux value was observed in the former and lowest value in yoke. It was depicted from the analysis that lines of contour were closer while passing through armature, upper region of former and contact area between them having opposite direction at the ends of former. Flux lines were observed to be directed along the same direction through cover plate and yoke leading to larger holding force generation. Flux lines passed through both the upper and lower regions of yoke base plate having minimum magnetic force is minimal at lower region of former and maximum force at upper region. Flux due to permanent magnet was opposed and canceled by electromagnetic flux at the time of coil excitation using inverse current. Therefore the closer lines were observed at lower region of former with different orientation at both ends. Flux generated before and after coil excitation was observed to be oriented in similar direction at

yoke, yoke cover plate, base plate and lower region of former. The armature holding force was observed to be negligible due to minimal flow of flux and differently directed flux at both ends of armature. The fringing was maximum when armature was at the equilibrium position. The flux through armature, yoke and yoke cover plate was directed in the direction of upper region of former while oppositely directed flow was observed in former lower region, yoke lower region and yoke base plate leading to minimum holding force.

Increasing the inverse current decreases the holding force with optimal current value of 1500Aturn for armature release. Increasing the current value from 1500Aturn lead to rise in holding force due to the dominance of electromagnetic flux over the permanent magnet reluctance decrease. A voltage pulse of magnitudes 12V and 24V with step of 1.5ms was applied in the simulation of current transient response. The input voltage of 24V power source resulted in rise of the current by 64% with peak value of 29A as compared to 12V power source having peak value of 6.5A. The results of current signal for both 12V and 24V step input are shown in Fig. 3.

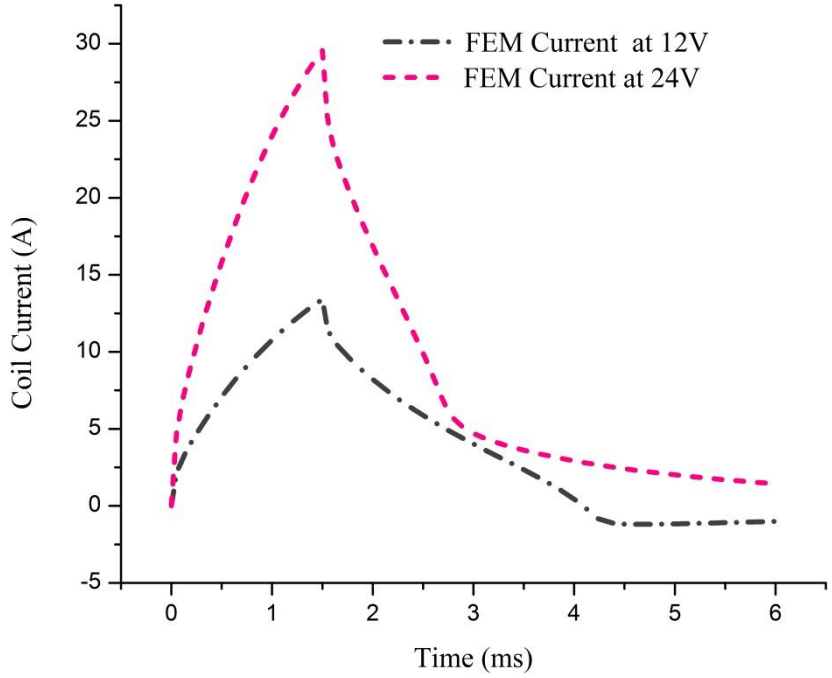

Figure 3 FEM Coil current transient responses at 12V and 24V

The slope of current response was steeper during the charging period while current discharging was gradual resulting in residual coil charging in the case of pulse time lower than

1.5ms. The higher voltage value lead to steeper current slop currents and larger energy dissipation. The power consumption value obtained from the analysis for release and catching of valve at current of 2000Aturns for generating 200N force was 156W.

3.4 Experimental Methodology and Apparatus

3.4.1 MHVA prototype fabrication

The MHVA was designed for large force potential over armature reciprocating span of 8mm having transient time of 6ms. Two similar precompressed linear springs were employed to provide the smooth and fast transient response leading to reduction in energy consumption. Universal Tensile Machine was utilized to obtain the stress strain curve for the springs. The springs were selected based on natural frequency requirement to maintain the engine speed of commercial engines of about 5000 to 6000 rpm. The dimensional parameters of spring were confirmed using the measuring devices such as vernier calipers. The spring constant value was 18.82 N/mm obtained by performing linear regression on stress strain curve obtained from testing on ultimate tensile testing machine and viscous damping coefficient was calculated from parameter identification of free oscillating under damped system. The experimentation of assembly was performed on dynamic test rig. The expression representing the freely oscillating under damped system is shown in Eq. (3.12)

$$F(x) = Ae^{-\xi\omega_n t}\, sin(\omega_d t - \theta) \tag{3.12}$$

The values of parameters A, ξ, $\omega_{n,}$, ω_d, θ were 3.26, 0.072, 441.1 rad/s, 439.6 rad/s, 1.669 rad were obtained from curve fitting the experimental data as shown in Fig. The viscous damping coefficient was calculated to be 3.559 Ns/m from the Eq. (3.13) given below.

$$c = \xi\sqrt{mk} \tag{3.13}$$

Armature assembly consisted of two parts including male and female stem joined together with the use of external and internal threads. Former consisted of a shaft and nut with two brass bushes to align the armature in the hole of 8mm. Edged one end of former supported the permanent magnet and the other end was fastened with screw to the other former part acting as a bolt. The whole former assembly was bolted to brass plate. The brass plate fastened the whole assembly to the rig for testing. The combined assembly of former and brass plate was bolted to

yoke and yoke cover plate with M3×6 bolts fixing the coil bobbin. The compact coil winding consisted of two coils having 200 turns each having wire diameter of cross section of 1.4mm. The winded bobbin was assembled on the former assembly by slip fitting and fixed by yoke cover plate. Two solenoids utilized for valve actuation consisted of coils in parallel orientation assembled to amplify the effect of both coils. The coil resistances for parallel coils pair of both upper and lower solenoids were measured to be 0.34 ohms and 0.37 ohms respectively and the overall resistance calculated was 0.35 ohms. The values of frequency for outer and inner coil pairs of both upper and lower solenoid were obtained to be 1.472MHz, 637.5 KHz and 1.463 MHz, 584.8 KHz respectively. Inductance values for outer and inner coils pair of both upper and lower solenoid were calculated to be 3.1046μH, 7.168μH and 3.1237μH, 7.814μH respectively.

3.4.2 Electrical Equipment

To achieve various current and voltage requirements for static testing, the power supplies were utilized in parallel and series combinations. With the combination of power supplies, the output voltage and current values achieved were 12V and 24V with 50A current.

By controlling MHVA current excitation, the steady state force requirement was achieved. BTN7971B integrated circuit consisting of half bridge configuration was integrated with data acquisition of actuator for the control of current.. The IC has high current 60A with maximum input voltage of 45V. The actuator coils were excited in one direction keeping U1 and U3 MOSFET from combination of two IC turned on and reverse excitation was achieved by turning U4 and U2 MOSFET on. The diodes prevented excess voltage build up at each MOSFET. The configuration of H-bridge design lead to achievement of +12, 0 and -12 V having maximum driving frequency of 20kHz for purpose of pulse width modulation. IC 74LVC245 was supplied 5V providing the driving signal from data acquisition system supplied to BTN7971B combination.

An eddy current sensor having a probe with power and amplification unit was utilized for the accurate position measurement of armature. A thin sheet of 50mm diameter and 1mm thickness made of tin was used as metal target. Eddy current was induced in the target metal with the generation of constantly changing magnetic field. Field generated by eddy currents opposed magnetic field of probe. By displacing the probe and target, the change in magnetic field was sensed generating an output voltage directly related to change of displacement. Before

experimentation, the sensor was calibrated. The lead screw attached to armature stem was used to generate the displacement of armature stem. By applying linear regression on the experimental data using position voltage function, the position was calculated corresponding to particular voltage. The voltage potion function used was Position = 2.0242×Voltage - 0.0573.

The static analysis of hybrid actuator involved the variation of holding force at different values of constant current excitation. A load cell having load bearing capacity of 200 kg was employed for force measurement for both cases of compressive and tensile loading. The load cell was bolted to load cell plate and calibrated before starting experimentation. The internal circuit of a load cell consisted of four strain gauges combined in Wheatstone bridge configuration with DC voltage supply. One end of armature stem was screwed to load cell and load discs were placed on armature putting load on force transducer and forced measurement was obtained on digital weighing scale. Linear regression was applied on the experimental data providing the voltage mass function to be Mass = 37.712×Voltage - 0.1476.

A Hall-effect current sensor was employed to measure the current by passing magnetic field generated due to flow of current through semiconductor having steel yoke. Current and voltage corresponding to magnetic field magnitude were generated with passage of current through semiconductor. The sensor contained a feedback loop based on operational amplifier and coil to prevent non-linearity of yoke and semiconductor producing opposing flux in yoke in proportion to flux generated by semiconductor. By allowing the current from operational amplifier to pass through a resistor and multi-turn loop of wire around yoke, a contour flux was produced. The calibration of current sensor was done after connecting the sensor to power supply with current input to coil as reference. The generated voltage corresponding to input current was logged by data acquisition system. By applying linear regression, two current voltage functions obtained were Current=168.67×Voltage+0.6386 and Current= 11.56×Voltage+6.1302.

The data acquisition system employed consisted of data acquisition module having graphic user interface and USB compatibility. The system has 16 single ended analog inputs having maximum sampling rate of 1.25MS/s with single channel and 1MS/s with multichannel input. The voltage measurement range was ±10V with 1520uV resolution. There were 4 Counter/timers with resolution of 32 bit to control the timing of actuator. The analog input was used for force, position and current sensor input.

3.4.3 Static and Dynamic Test Rigs

The assembly of hybrid actuator was fastened to static test rig in way that armature displacement was in vertical direction. The rig comprised of three holding plates having 10mm thickness, with the top and central plates for valve and lower plate for supporting load cell of 10mm thick. The two side walls supported the holding plates using M6×10 Allen bolts. The whole test rig assembly was supported using rubber damper fixed to the ground with two chuck nuts. Both the solenoids were tested for static experimentation. The position sensor was assembled at the top and the load cell at the bottom of armature stem. Armature was displaced from one position to another using the lead screw for the analysis of holding force for each position at different values of constant current. An averaged value was taken of thousand values of force at each displacement varied from 0.5-4mm to achieve reasonable precision. The input current was turned to zero before varying the displacement of armature. The force sensor was powered by 220VAC while the other sensors including power module, position sensor and current sensors were powered by DC power supply. The analog data obtained from different sensors was logged in computer using data acquisition system. The variation of holding force with air gap observed during experimentation is plotted in the Fig. 4. The experimental force behavior was reasonably close to the FEM force behavior.

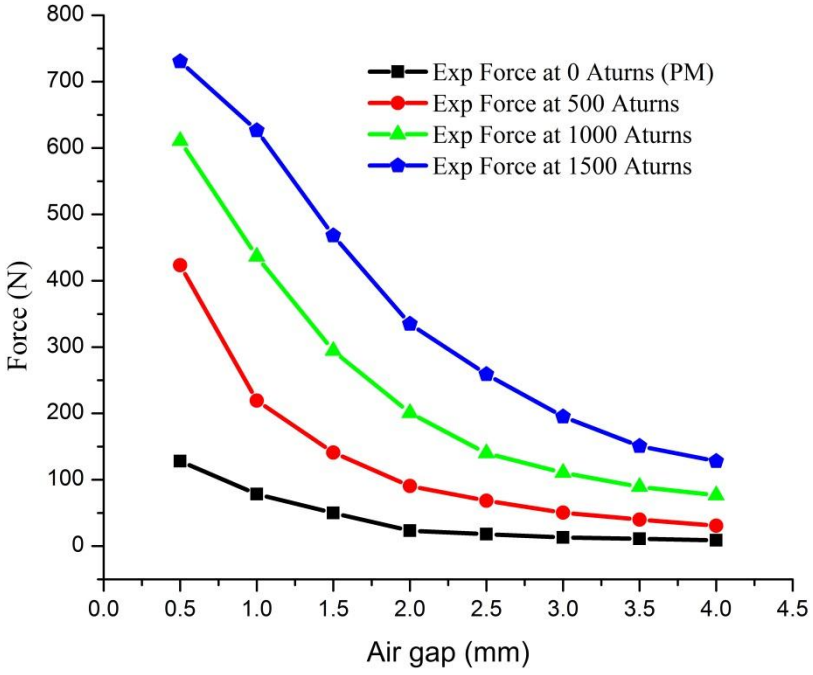

Figure 4 Experimental Force response with air gap (PM and EM)

Inverse current excitation was input to the modified hybrid actuator for experimentation on the basis dynamic and transient analysis. The current transient response was obtained for step input voltage signal of 12V and 24V without current control for the actuator. Quick rise in the current was observed for larger air gaps having low inductance value of magnetic circuit. To limit the current magnitude, the duration of input voltage step was set to be 1.5ms for large displacement of armature. The coil current signal transient response observed during experimentation is plotted in the Fig. 5. The current signal obtained during experimentation was comparable with the current response obtained using FEM analysis.

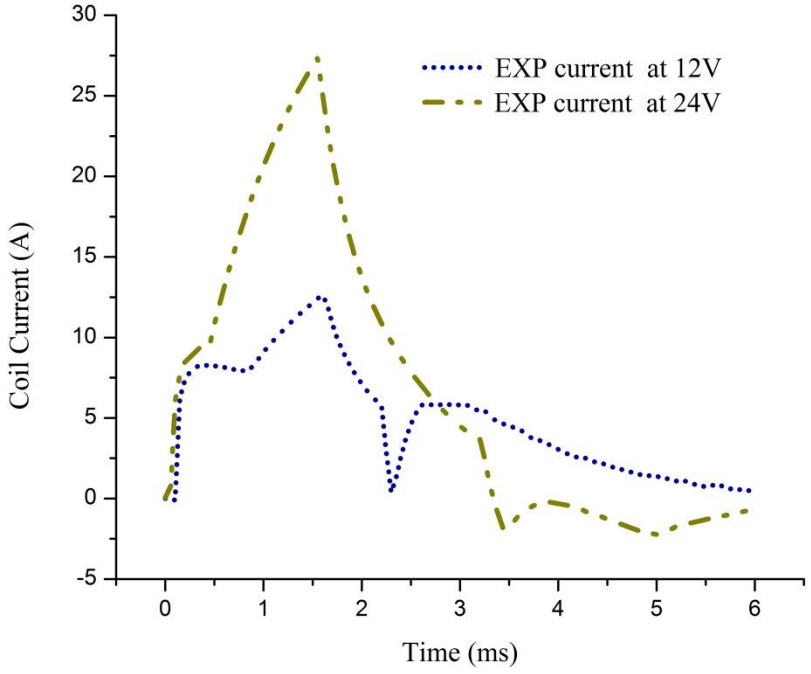

Figure 5 Experimental coil current responses at 12V and 24V

The force sensor, lead screw and load cell holding bolt were removed for free oscillation of armature through the reciprocating span and two precompressed springs were included in the setup, fastened to brass plate with help of cotter and valve retainer. Initially the armature was kept at equilibrium position with help of precompressed spring and lead screw. The dynamic experimentation included operation of releasing or catching of armature at one time considering opening or closing solenoid operation. The most concerned parameters for the dynamic testing involved physical property values at low air gap conditions influencing the landing velocity of

armature. For the dynamic analysis, the feedback loop of position sensor and current sensor was required. For dynamic testing pair of coils are separately triggered by power driver circuit thus two current sensors are employed to sense the currents in inner/outer coils. Two current sensors were employed for current magnitude determination in outer and inner coil separately.

3.5 Summary

The chapter discussed basic design considerations, FEM analysis, fabrication and assembly of experimental setup of modified hybrid actuator prototype. The design of actuator was validated using FEM analysis before prototype development and experimentation. Working, calibration and assembly of different types of electronic sensors including position, force and current sensor were discussed. The assemblies of static and dynamic test rigs were discussed. The designed hybrid actuator was energy efficient with low coil inductance and improved response time. The results obtained from the experimentation and FEM analysis were utilized to develop lumped parameter model of hybrid actuator without computation burden of FEM technique and providing overall dynamic response of the actuator within a reasonably less time. The LPM can further be used to develop control strategies leading to improve the hybrid actuator design and experimentation can be done using control implementation.

CHAPTER 4: MODELING OF MHVA

4.1 Introduction

A mathematical model of hybrid camless actuator system is developed based on set of mathematical equations. The selected equations were developed on the basis of scientific principles and theories. The model presented in this study describes the behavior of modified hybrid actuator on the basis of important physical properties governing the working of actuator system. The model included the electrical, magnetic and mechanical subsystems integrated to develop lumped parameter model of the overall system. The electrical subsystem modeled the current signal for working of electromagnet based on input step voltage signal. The magnetic subsystem provides the modeling of electromagnetic force generated by the electromagnet with current signal as input to the subsystem. The mechanical system models the spring force and the damping included in the system. The net force obtained by subtracting electromagnetic force from spring and damping force is used to obtain velocity and position by integrating the differential equation. In the mechanical system, electromagnetic force is the input and armature position and velocity as output.

4.2 Theory of mathematical modeling

A mathematical model is developed to express the behavior of a static, dynamic, statistical or other system in language of mathematics. The benefits of mathematical model include the effects of different physical components and behavior changes by varying the quantities of important physical properties termed as parameters. The mathematical model presents the overall behavior of the system on the basis of differential equations or other set of equations and valid initial conditions without the complex and lengthy methodology of finite element analysis. The model helps in thorough understanding of working of a system, improvement in the system by control designing and implementing on the basis of mathematical model. The assessment of model includes comparison of model with experimental results providing a way of confirming the model depicting the behavior of a real world system. There is a certain limit to which the mathematical model can predict real life phenomenon and it can include non-linearities upto a certain extent.

Before the modeling is done, it is important to decide the level of information or detail to be included in the model known as abstraction process. The first step involved in methodology of mathematical modeling requires finding the physical quantities on which the behavior of system or device depend the most. A set mathematical equations involving the most effective physical parameters representing the subsystems is selected for the modeling of individual subsystems. The mathematical equations are selected on the basis of scientific principles such as conservation of momentum on which the system to be modeled is based. Every equation used in the modeling must be dimensionally consistent. Using the corresponding mathematical equations, curve fitting is performed using reasonable modeling software such as Matlab, Origin on the concerned experimental curves. The important unknown physical coefficients are identified using different mathematical techniques with iterative procedure. The physical parameters are identified for the all the subsystems and the individual subsystems are integrated with feedforward and feedback modeling using reasonable software such as S-Function of Simulink module available in Matlab software. With valid initial values of concerned parameters, the model provides the graphical representation of important physical properties affecting the overall working of the system. The mathematical model of system developed in this way is known as lumped parametric model. The curves obtained from the LPM are then compared with those obtained from experimentation performed before modeling. A reasonable comparison with negligible error between the experimental and modeled results verifies the lumped parametric model of the system.

4.3 Curve fitting

4.3.1 Theory of Curve fitting

The nonlinear fitting is an analytical technique used to determine the optimal parameter values which best describes the data. The technique of curve fitting includes the selecting a well-known mathematical function or writing a user defined function with reasonable initial values. The next step is performing the iterative curve fit ting procedure utilizing a reasonable algorithm to adjust parameter values that fit the data in the most optimal manner. The fitting procedure is stopped when difference between the data to be fitted curve is minimum and the stopping criterion is reached to get the best fit.

There are different algorithms available for curve fitting implementation on a particular set of data points. These algorithms for the curve fitting include Levenberg–Marquardt algorithm and

trust-region-reflective approach. The Levenberg-Marquardt algorithm is an iterative optimization methodology involves finding of the minimum of a function and the minimum is expressed as the summation of squares of nonlinear functions.

$$F(x) = \frac{1}{2}\sum_{i=1}^{n}[f_i(x)]^2 \tag{4.1}$$

$$(J_k{}^T J_k + \lambda_k I)p_k = -J_k{}^T f_k \tag{4.2}$$

Here J_i(x) is the Jacobian of f_i(x), p is the solution of the equations, λ_k are nonnegative scalars and I denotes the identity matrix. The curve fitting methodology is a standardized optimization incorporates a combinative approach of steepest descent and the Gauss-Newton method. The gradient descent approach involves updating the solution values resulting in smaller value of function. The Levenberg–Marquardt technique selects a value from two approaches gradient descent and Gauss Newton during each iteration for updating the solution. The selection of value from the two approaches is based on a parameter known as algorithmic parameter, λ and this parameter is a non-negative parameter resulting in smoothing of the graph. With smaller λ which is closer to the optimal value, Gauss-Newton approach is used and with larger value of λ, gradient descent is used for updating the solution. Trust-region methodology is used for constrained numerical optimization of nonlinear problems. In this technique, a region is specified around the best possible solution within which a specific model is utilized to estimate the objective function. The trust-region method identifies the step size before the stepping towards improvement and the reasonable estimation of objective function is achieved with required minimization of the concerned parameters. A trust region method has a region around the current search point, where the model used to estimate objective function is given in Eq. (4.3).

$$q_{k(p)} = f_{(x_k)} + \nabla f_{(x_k)}{}^T p + \frac{1}{2}p^T B_k p \tag{4.3}$$

After choosing a step size, the function value is compared with predicted value obtained using above mentioned model in Eq. The ratio of actual and predicted model is given by Eq. (4.4). The value of ratio closer to 1 indicates good estimation of actual function.

$$\rho_k = \frac{\text{Actual reduction of f}}{\text{Predicted reduction of f}} = \frac{f(x_k) - f(x_k + p_k)}{q_k(0) - q_k(p_k)} \tag{4.4}$$

Different analysis softwares including MATLAB, Origin can be used to perform curve fitting on a certain data set or on multi-curve data. There are certain parameters to check the quality of fitting performed on a given data set and the technique known as goodness of fit. The optimal parameter value is achieved with minimizing value of reduced chi-square in an iterative manner. Using a scaling factor with the observed data leads to error in reduced chi-square value as the scaling factor also applies to the reduced chi-square value. A substitute of reduced chi-square is r square with reasonable determination of goodness of fit. If the r square value is nearer to 1 then the estimation of data set is good. R square value becomes erroneous with increasing the degree of freedom leading to poor insight of goodness of fit for the concerned data points. The adjusted r-square value is used instead of R square to account for the higher degrees of freedom.

The reduced chi-square is given in Eq. (4.5) with degree of freedom denoted as K. Here the chi-square is given by Eq. (4.6) with input variance, observed and calculated data points denoted by σ_i, O_i and C_i respectively.

$$\chi^2{}_{red} = \frac{\chi}{K} \tag{4.5}$$

$$\chi^2 = \sum_i \frac{O_i - C_i}{\sigma_i} \tag{4.6}$$

The R-square and adjusted r-square is given in Eq. (4.7). Here SSR, SSE and SST denote sum of squares of regression, sum of squares of error and total sum of squares. The mathematical relations representing SSR, SSE and SST are given in Eq. (4.10), (4.11) and (4.12). Here 'v' represents degree of freedom, 'n' and 'm' denotes response values and number of fitted coefficients and v=n-m.

$$\text{R-square} = \frac{SSR}{SST} = 1 - \frac{SSE}{SST} \tag{4.7}$$

$$\text{Adjusted R-square} = 1 - \frac{SSE(n-1)}{SST(v)} \tag{4.8}$$

$$SST = SSR + SSE \tag{4.9}$$

$$SSE = \sum_{i=1}^{n} w_i (y_i - \hat{y}_i)^2 \tag{4.10}$$

$$SSR = \sum_{i=1}^{n} w_i (\hat{y}_i - \bar{y})^2 \tag{4.11}$$

$$SST = \sum_{i=1}^{n} w_i (y_i - \bar{y})^2 \tag{4.12}$$

4.3.2 Curve fitting in Origin

The least square fitting was performed on the experimental force data using Origin software. Origin provides a comprehensive way to perform non-linear least square curve fitting of experimental data with arrange of mathematical functions. The force equation was used in the user defined function option of the non-linear curve fitting available in Origin was used to develop force approximations and physical parameters were identified. The non-linear curve fitting of Origin software utilizes Levenberg Marquardt algorithm for the fitting of mathematical model to the experimental data points.

The first step in the curve fitting is using the Function Builder option in the Origin to write a mathematical function with reasonable initial guess values. A proper name is given to the fitting function for further use in the non-linear fit option. Before writing the function, the independent and dependent variables, constant and parameters to be identified, are specified with proper alphabetical or Greek letters. Initial values of parameters and constants are set manually while writing the function body. Origin C can be selected as function type, if the function is to be defined using a code in the code builder workspace. After properly defining the function, the function builder window is closed and non-linear curve fit is opened in the analysis tab. In the non-linear curve fit window, user defined category is selected and function developed in the function builder is selected by name of function. After function selection, the data points are fitted with the corresponding function using fit until converge option. If the curve does not converge then the initial guess values of parameters must be changed and the procedure is repeated until the function fit to the data points.

Origin can be used to fit multiple curves using global fit option in the multi-data fit mode in the setting. The option of add all plots in the active page in the input data tab is selected to include all the curves for the analysis purpose. The individual curves can be fitted using independent fit option of multi-data fit model to determine independent values parameter for each data included in the analysis. The fitting of multiple data sets can be performed one after the other or simultaneously by adding all the curves in the active page. The multiple curve data can be fitted using global fit option with both the shared parameters and local parameter techniques. In the shared parameter fitting technique, one best fit value of each shared parameter is approximated for all the curves in the active page. In the local parameter fitting technique, separate values of parameter are approximated for all the curves in the active page. Origin provides a convenient way to select all the parameters as shared parameters and one or two parameters of choice as shared parameters and remaining as local parameters. Concatenate fit option is utilized for fitting data comprising of multiple runs of experiments under similar conditions known as replicate data. Concatenate fit mode performs sequential arrangement of all y-axis data points to fit them as single optimized curve.

4.3.3 Parameter identification and optimization

The finite element analysis was performed using the static conditions as used for the static experimentation and the simulations were executed using Ansys Maxwell. In this methodology, a model of hybrid actuator was first developed and the experimental model was fabricated in accordance with the model developed in Ansys Maxwell. The simulation performed under static conditions was done for one fixed value of current for displacement from 0.5mm to 4mm and in this way three fixed value of current were taken for the simulation purpose. The experimentation performed under same conditions as used for FEA provided the holding force due to electromagnet and permanent magnet. The holding force due to permanent magnet was obtained experimentally at current 0 Aturn with peak value of 128 N and lowest value of 8.7 N. the force due to electromagnet was obtained at the current value of 500, 1000 and 1500 Aturn with peak values of 423.5, 611 and 730.5 N. The experimentation was conducted for the armature displacement from 0.5mm to 4mm with interval of 0.5mm. For the stroke length other than 4mm region, the change in the holding force was observed to be negligible. Only 4mm stroke length was taken into consideration for the experimentation of force variation with corresponding displacement. The graph plotted between holding force and displacement of armature showed

similar decreasing trend of force from 0.5mm to 4mm for both cases of FEA and experimentation.

4.3.3 Linear system of equations

The mathematical equation selected for holding force approximation was a simplified equation without consideration of eddy current, magnetic saturation and flux leakage [16]. The equation for the inductance of coil was of the form as given in the Eq. (4.13).

$$L(x) = \frac{2\beta}{(\kappa - x)} \tag{4.13}$$

The parameters β and κ in the above equation are dependent on the number of turns, area and lengths of the path of flux and magnetic permeabilities of the air and iron core of the coil. The equation for holding force can be obtained by differentiating the coenergy equation given in the Eq. (4.14) with respect to position.

$$W(x, i_c) = \int_0^{i_c} \lambda(x, \xi) d\xi \tag{4.14}$$

The parameter λ is the flux leakage which is represented in the Eq. (4.15) as

$$\lambda(x, \xi) d = L(x) i \tag{4.15}$$

After the differentiation of coenergy function, the equation of holding force obtained is given in the Eq. (4.16).

$$F_m(x, i_c) = \frac{\beta {i_c}^2}{(\kappa - x)^2} \tag{4.16}$$

The above equation of force was used to develop the force model based on the experimental results of force variation with respect to air gaps or displacement. The equation for holding force is well suited for unsaturated regions of the actuator assuming the permeability of the material to be constant. The physical parameters β and κ are determined by the least square fitting of experimental data of force variation with armature position. The optimized values of both the parameters for all the three data sets are calculated using Levenberg–Marquardt technique in origin. These optimal parameter values are obtained using multicurve fitting in origin utilizing

global fitting with sharing of parameter values for all the data sets. The optimized values of parameters are given below.

$$\beta = 0.28\, N \frac{mm^2}{A^2}$$

$$\kappa = 0.00104\, mm$$

The individual parameter values can also be obtained without sharing the parameter values for all the data sets. Mathematical approximation of force generated by permanent magnet can be conveniently and comprehensively obtained using the mathematical expression developed for electromagnetic force approximation. The effect of permanent magnetic force is included in the determined parameter values as the fitting is performed on force data including both electromagnetic and permanent magnetic force. The curve fitting performed on individual force curve without sharing the parameter values is shown in the graph in the Fig. 6.

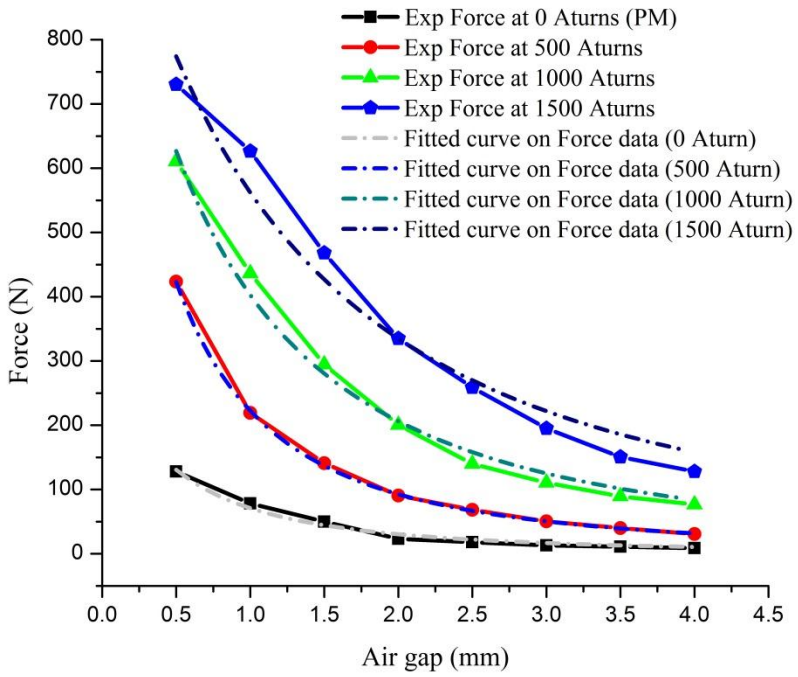

Figure 6 Curve Fitting of Static Experimental Force Data (linear system)

4.3.3 Nonlinear system of equations

Least square curve fitting was also performed on the experimental force data using a non-linear system of equations to verify the accuracy of developed LPM. The system of equation includes the magnetic saturation effects leading to an improved model as compared to the first model developed in this study. The non-linearities incorporated in this system leads to better control implementation. Non-linearities of flux linkage are mathematically represented by Eq. (4.17).

$$\lambda(x, i_c) = \lambda_s(1 - e^{-i_c f(x)}) \tag{4.17}$$

Here λ is flux linkage of the coil, λ_s is the saturated coil flux linkage and i_c is the coil current. The function $f(x)$ in Eq. (4.17) is used to relate varying armature position and is given in Eq. (4.18).

$$f(x) = \frac{2C_1}{C_2 - x} + C_3 \tag{4.18}$$

Here the parameters C_1, C_2 and C_3 are determined from experimental data. The function $f(x)$ quantifies the severity level of saturation and λ_s gives flux linkage values at saturation. The electromagnetic force can be derived from co-energy function given in Eq. (4.19).

$$W_c\,(x, i_c) = \int_0^{i_c} \lambda(x, \xi) d\xi \tag{4.19}$$

Differentiation of co-energy function gives following expression.

$$F(x, i_c) = \frac{\partial W_c(x, i_c)}{\partial x} \tag{4.20}$$

The electromagnetic force expression is obtained by substituting Eq. (4.17) into Eq. (4.20).

$$F(x, i_c) = \frac{\lambda_s f'(x)}{f^2(x)}\left[1 - [1 + i_c f(x)]e^{-i_c f(x)}\right] \tag{4.21}$$

Here $f'(x)$ is given by following expression.

$$f'(x) = \frac{2C_1}{(C_2 - x)^2} \tag{4.22}$$

The parameters λ_s, C_1, C_2 and C_3 are determined by least square fitting of experimental force data under constraints. The optimized parameter values obtained for all the data sets are given below. The curve fitting is shown in Fig. 7.

$$C_1 = 0.0070\ mm/A$$

$$C_2 = 0.0604\ \text{mm}$$

$$C_3 = 0.000218\ A^{-1}$$

$$\lambda_s = 0.046\ Wb$$

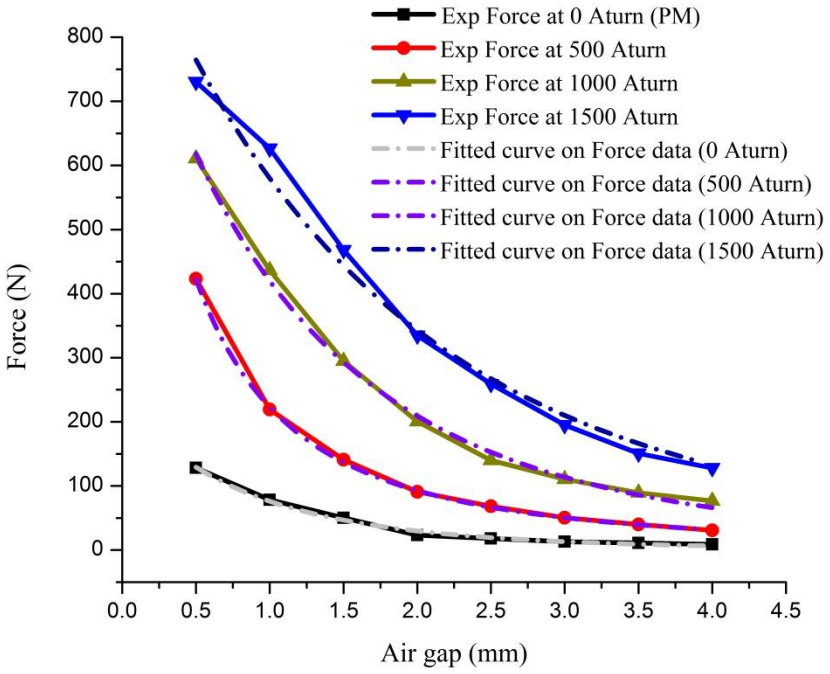

Figure 7 Curve fitting of Static Experimental Force Data (nonlinear system)

4.4 Lumped parameter modeling

Lumped parameter modeling provides simple explanation of behavior of a real life multi-physic system comprising of a set of distributed subsystems such as electrical system in combination with mechanical system or fluid dynamic system and chemical kinetic system under

certain constraints. Lumped parameter modeling is an effective methodology in the modeling of systems combining multiple physical phenomena. The lumped modeling is based on set of mathematical equations describing the behavior of different physical phenomena and integrating the subsystems to develop a sense of overall behavior of main system. The set of mathematical functions for the development of lumped parameter model is selected based on certain physical laws such as law of conservation of momentum governing various phenomena. Each subsystem in the lumped system model affects the behavior of other system. In this way, a comprehensive analysis of dependence of various physical properties on the combined system and the effect of physical quantities on one another can be performed. It involves less complexity and computation burden as compared to finite element analysis methodology for designing and analyzing systems based on different scientific phenomena. The lumped parameter model developed for a physical system can be used to implement different control strategies to obtain desired behavior of important physical properties leading to improvement in the system making it more efficient and robust.

In this study, a lumped parameter model is developed for a multi-physic system designed and fabricated to develop effective and energy efficient camless hybrid electromagnetic actuator for intake and exhaust valve operation of automobile engine. The multi-physic system designed for hybrid actuator includes electrical subsystem, magnetic subsystem and mechanical subsystem. The three subsystems are modeled desperately using different mathematical functions representing the behavior of corresponding subsystem and then integrated to develop a single model capable of predicting the overall dynamics of valve actuation system. The individual models of subsystems are developed in the S-function of Simulink module of MATLAB. Before the modeling the subsystems, important physical parameters are determined using least square curve fitting performed on experimental force data under static conditions. The determined parameters play a vital part in predicting the dynamics of subsystems and the development of mathematical models of subsystems. The individual subsystem models are integrated using input and output ports according to subsystem requirements to develop lumped model in S-function. The detailed description of each subsystem model is given in the coming sections.

4.4.1 S-Function development

The user defined option available in the library of Simulink module of S-Function is utilized to solve the mathematical equations for development of limped parameter model of modified hybrid actuator. The S-Function can be used to build a custom or user defined block in Simulink as compared to build-in blocks which are limited to a specific task or action. It can be used to develop a system based on set of mathematical equations, analyzing and solving the mathematical equation to describe the behavior of a modeled system. It can be used to solve complex differential equations and can represent the results of a set of mathematical equations in graphical animations for clear and comprehensive explanation of a continuous, discrete or hybrid system. It can incorporate both m-file code developed in MATLAB and code developed in C, C++ and Forton programming languages. The software provide a convenient way to develop a step voltage signal of 12V and 24V through signal builder available in the block library of Simulink to be used as an input to the electrical subsystem model development. The S-Function is an important tool for enhancing the capabilities of Simulink module. The S-Function tool utilizes a programming language description to operate a Simulink block in MATLAB. The S-functions are compiled with the use of mex utility as MEX files and these functions are dynamically linked subroutines automatically loaded and executed with the help of MATLAB execution engine. S-functions uses a calling syntax known as the S-function API facilitating the interaction of function with the Simulink engine as the interaction of built-in functions with Simulink engine. The general form of S-Function can facilitate the use of continuous, discrete and hybrid functions in an effective and comprehensive manner.

The understanding of S-Function is based on the knowledge of working of a block in Simulink module. The mathematics of a block must be understood in order to develop a complete sense of Simulink block working and ultimately the working of S-Function. A block in Simulink comprises of three sections including the input required by the system, states of function and the expected output of system. The S-Function block in the Simulink is executed in steps including initialization, simulation loop, functions for computation. In initialization step, Simulink integrate library blocks to form a model, types of data and time range for the evaluation, parameter determination, separates and disseminates memory. Simulink then enters a loop with each cycle to be called as simulation step. The Simulink executes each block one after

the other in a systematic manner. The execution of every block includes functions for block state, derivative and output computation.

An S-function employs a number of S-function callback techniques required for task completion at every simulation stage. Tasks to be completed by S-Function include initialization, computation of next sample hit, output calculation, discrete state update and integration. The initialization stage includes initialization of a structure containing the necessary information about S-function known as SimStruct. It also includes selecting the appropriate number of input and output ports, selecting a reasonable sample time and selecting size arrays for simulation purpose. The second stage involves the calculation of next sample hit in accordance with the variable sample time block. The next stage incorporates the computation of output within the time range provided. Then the next step includes the updating of discrete states for the next time step of simulation loop as all the blocks can be evaluated once in a time step. The next step is required for the case of continuous data and it involves calling of output and derivative of S-function in the given time step. This stage includes the computation of states of functions which means solving the derivatives with respect to given initial conditions provided in the initialization step.

4.5 Electrical subsystem model

The electrical model represents the dynamics of coil current which is an important input parameter for the working of modified hybrid actuator. The electric model was developed based on the differential equation combining physical properties including the inductance and resistance of coil, input voltage. The physical parameter values were used in the differential equation for determining the current variation with respect to time. The input step voltages of 12V and 24V magnitude were used in the modeling of current required for the working of electromagnets of actuator. The overall resistance value is 0.35 ohms which is the same as calculated for prototype.

4.5.1 Linear system of equations

The equation of circuit representing rate of change of flux based on the Kirchhoff's Law and Faraday's Law for the electrical subsystem is given by Eq. (4.17).

$$\frac{d\lambda}{dt}(x, i_c) = v_c - R_c[i_c + i_e] \tag{4.17}$$

$$\frac{di_e}{dt} = \frac{1}{L_e}\left[v - R_c[i_c(\lambda, x) + i_e\ ]\right] - R_e(x, i_c)i_e \tag{4.18}$$

$$i = i_c + i_e \tag{4.19}$$

The effect of eddy current is neglected in the modeling of electrical subsystem for the actuator to avoid complexity and burden of calculations. Without the effect of eddy current the flux expression is given in Eq. (4.20).

$$\frac{d\lambda}{dt}(x, i_c) = v_c - R_c i_c \tag{4.20}$$

The above equation is combined with the inductance function and a differential equation is developed to approximate the transient behavior of current. The current signal obtained by integrating the differential equation will then be used as an input signal for electromagnetic force generation by the electromagnet. The inductance function was developed without considering the effects of eddy current, magnetic saturation and flux leakage [16], which is given below in the Eq. (4.21).

$$L(x) = \frac{2\beta}{\kappa - x} \tag{4.21}$$

The differential equation representing the transient behavior of coil current without incorporating the effect of eddy current is given by Eq. (4.22).

$$\frac{di_c}{dt} = \frac{\kappa - x}{2\beta}(v_c - R_c i_c) - \frac{\dot{x} i_c}{\kappa - x} \tag{4.22}$$

The above equation can also be written in another form as given below in Eq. (4.23).

$$\frac{di}{dt} = \frac{\lambda}{2\beta}(\kappa - x) \tag{4.23}$$

Here the value of λ can be obtained by integrating the differential equation involving λ variation with time given in Eq. The parameters β and κ were obtained by least square fitting of static experimental force data. The coil voltage required for obtaining the transient current is

based on step input signals of magnitude 12V and 24V. The overall resistance is 0.35ohm for parallel combination of inner and outer coils of upper and lower solenoid.

4.5.2 Nonlinear system of equations

The coil dynamic equation derived with saturation effects for non-linear system used in [29] is given below. The non-linear system of equation with four fitted parameters is also used to develop LPM in a similar manner as the relatively simple system of equation with two fitted parameters. Eddy current effect is neglected using nonlinear system for LPM development.

$$\frac{di_c}{dt} = \frac{e^{i_c f(x)}}{\lambda_s f(x)}[v_c - (R_c i_c) - \lambda_s f'(x) x \imath_c e^{-\dot{\imath}_c f(x)}] \tag{4.24}$$

4.6 Magnetic subsystem model

The holding force generated by both electromagnets and the permanent magnets is utilized to attract the armature towards the coil and hold it firmly after a contact is developed between the coil and armature. At the beginning of the operation of valve opening and closing, the permanent magnet provides the holding force to the armature for latching to the lower solenoid seating position. At this position, the spring force is smaller than the holding force generated by the permanent magnet due to its reluctance. The spring force of two springs assembled one at either side of armature; keep the armature fixed to the lower seating position to keep the valve open in the absence of any external force. The inverse charging current is applied to reduce the flux of permanent magnet reducing the force due to permanent magnet and allowing spring force to release the armature form seating position and moving it to the closing valve position. The inverse current is removed as the armature move through the equilibrium position and charging current generated by upper solenoid helps in attracting the armature to the upper seating position. The charging current is removed as the armature reaches the upper seating position and at the same time the permanent magnetic provide the necessary holding force keeping the armature in the fixed seating position for the closing of valve. In this way, the valve opening and closing operation is carried out and the cycle continues as long as excitations are provide by the solenoids.

The holding force experimentation was performed with three different excitation current values of 500, 1000 and 1500 Aturn. The force due to permanent magnet assists in latching the

armature at seating positions for both opening and closing of valve. The application of permanent magnet is an important addition in the design and development of camless electromagnetic actuator as it reduces the energy consumption required for operation of electromagnetic actuator. In the absence of permanent magnetic, excitation of solenoid will be required for latching of armature to the seating valve positions. The armature displacement is carried out in the span length of 8mm. The experimentation for evaluation of holding force was conducted for a stroke length starting from 0.5mm to 4mm as the force variation was significant only in 4mm length and insignificant for the remaining length. The span length from 0-0.5mm is not included as force generated due to current excitations deflected the armature at seating position leading the force magnitude to unpredictable variations. The same conditions were utilized in the Ansys Maxwell before experimentation to observe the variation of holding of force for both permanent magnet and electromagnet. The results of both FEA methodology and experimentation were in agreement with each other.

4.6.1 Linear system of equations

The force model developed on the basis of assumption of no magnetic saturation, flux leakage and eddy current. The electromagnetic inductance on the basis of these assumptions is mentioned in Eq. (4.13). The force equation is obtained with the assumption of no magnetic couplings and is given differentiating the coenergy function with respect to armature position given in above Eq. (4.14). The force equation is given by Eq. (4.16). The coefficients β and κ are determined by least square fitting performed on the experimental static force data using Origin software. The multi-curve data was fitted using the force function and the parameters β and κ are shared for all the active curves using global fit approach.

4.6.2 Nonlinear system of equations

The force model developed incorporate nonlinearities including magnetic saturation effect. The eddy current is neglected in this model to avoid complication. The flux linkage expression incorporating the saturated flux linkage is given in Eq. (4.17). The function *f(x)* indicates the severity of saturation and varying armature position. The electromagnetic force obtained by combining flux linkage and *f(x)* is given in Eq. (4.21). The optimized parameters λ_s, C_1, C_2 and C_3 are obtained by least square fitting of experimental force data under constraints.

The transient model of holding force due to permanent magnet and electromagnet is developed utilizing S-function of Simulink module of MATLAB software. The input parameter for the magnetic subsystem developed in S-function representing the transient variation of armature holding force coil current. The coil current transient response was generated by electrical subsystem model developed in the S-function. The output generated by the magnetic subsystem is the force transient response which increases with increasing both the coil current excitation and armature displacement values. The force transient response showed peak force magnitude for smaller air gaps and force decreases for larger air gaps. At quite low air gaps, the armature deflects to minimize the nominal air gap which is assumed to be rigid. This leads to erroneous force readings at lower air gaps.

4.7 Mechanical subsystem model

The armature position variation with time is modeled with single degree of freedom as mass spring damping system. The span length of armature displacement is 8mm between the two armature seating positions. The spring design parameters required for calculation of important parameters including damping coefficient and spring stiffness are given in the experimental setup chapter discussed previously.

The basic theory of mass spring system includes two types of systems. One system has fixed based with applications in building structures and the other system has base excitations with applications in automobile suspension system and seismic sensors. The system with fixed base is used to model forced and damped mass spring system of dynamics of armature of camless electromagnetic actuator. This model included the effects of spring force, viscous damping force and external force which is the holding force generated by both permanent magnet and electromagnet. The value of spring constant ‘k’ for the spring used in the experimental setup is 18820 N/m and the value of viscous damping coefficient ‘c’ calculated for the system is 3.559 Ns/m. The data of holding force F_m is obtained from the output of magnetic subsystem modeled in S-function of Simulink module. The gas pressure on the valve face is ignored in the dynamic analysis of armature to avoid cost of experimentation and complexity. The mechanical subsystem is developed using S-function of Simulink module of MATLAB as the other subsystems including electric and magnetic subsystems are modeled. The differential equation representing the forced and damped armature spring system is given by Eq. (4.24).

$$m\ddot{x} + c\dot{x} + kx = F_m \tag{4.24}$$

The armature dynamic equation is same for both linear and nonlinear systems used to develop LPM. Solving the differential equation using the S-function of Simulink module gives armature displacement as the output of the mechanical subsystem of lumped parameter model. Differentiating the output of mechanical subsystem gives armature velocity and further differentiating the armature velocity data gives armature acceleration. The armature position, velocity and acceleration values are feed-backed to the mechanical subsystem. The armature position and velocity is feed-backed to the magnetic system and armature position and velocity are feed-backed to the electrical system. The output of mechanical system which is armature position is an important parameter and it can be utilized further to implement control strategies for improving the modified hybrid actuator design. Different control strategies including PID controller, fuzzy controller and other control techniques can be developed for further improvement in the design of hybrid actuator. The mathematical model developed in S-function provide basis for the control implementation to achieve further lower velocity at the armature seating position and wear, tear issues can be reduced for long term application of actuator in the commercial automobile engine.

4.8 Summary

The LPM reduces time and burden of computation as compared to both the experimentation and FEM and can be used to implement control strategies. This chapter includes the step by step methodology for the development of LPM based on experimental results and actuator specifications of previous research work by J. Aslam *et al* [41] and linear and nonlinear system of mathematical expressions representing the coil current, force required for the movement of armature and dynamics of the armature. The curve fitting performed on experimental force results provide physical parameters used in the modeling of individual electrical, magnetic and mechanical subsystems. The LPM for both the systems are developed using S-function in Simulink module of MATLAB using the identified best fit physical parameters and other physical properties having same values as used in experimental test bed.

CHAPTER 5: RESULTS AND DISCUSSION

5.1 Introduction

The results of two LPMs developed for MHVA using linear and nonlinear system of equations are presented in this chapter and a comparative study is performed to validate the LPM results in comparison with FEM and experimental results of previously performed study. The physical properties including coil current, force for movement of armature within 8mm stroke length, armature displacement and velocity are modeled in LPM and are compared with FEM and experimental results of previous research work.

5.2 Current and force response

The current model with combined effect of electromagnet and permanent magnet is developed using lumped parameter technique in Simulink module of MATLAB. The behavior of current and force is observed for two different step voltage input signals of 12V and 24V with the step of 1.5ms. The air gap value of 0.5mm is reasonable to obtain realistic values of current and force. The current transient responses for both the system of equations are obtained at 0.5mm for the time constrained voltage and the comparison of experimental, FEM and LPM gives good agreement between the corresponding responses. The LPM current peak for linear system compared with FEM and experimental at 12V responses are in good agreement within 10% error. The current peak errors are within 15% range for 24V signal. The current rise is dependent on duration of voltage signal, inductance and overall resistance of combination of coils. The current peak increases with increasing the air gap and force peak decreases due to lowering of inductance magnitude at higher air gaps. At smaller air gaps, the current and force models become erroneous due to deflection of armature to reduce nominal air gap which is assumed to be rigid during modeling. The input voltages signals used for LPM current responses obtained using linear and nonlinear system of equations are shown in Fig. 8 and 9. The current response using simplified linear system for both 12V and 24V signals are shown in Fig. 10 and 11. The corresponding force responses are given in Fig. 12.

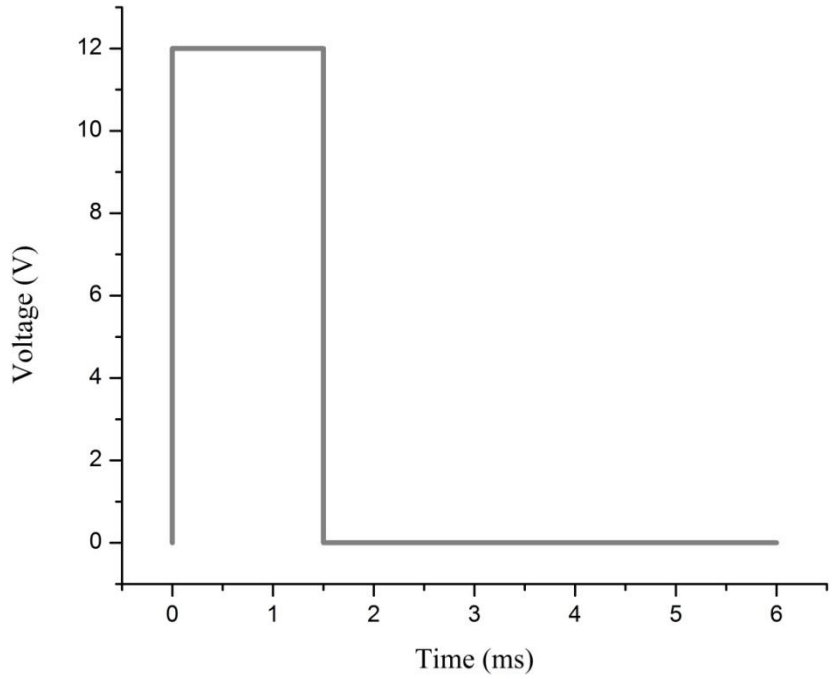

Figure 8 Input voltage Signal for LPM (12V)

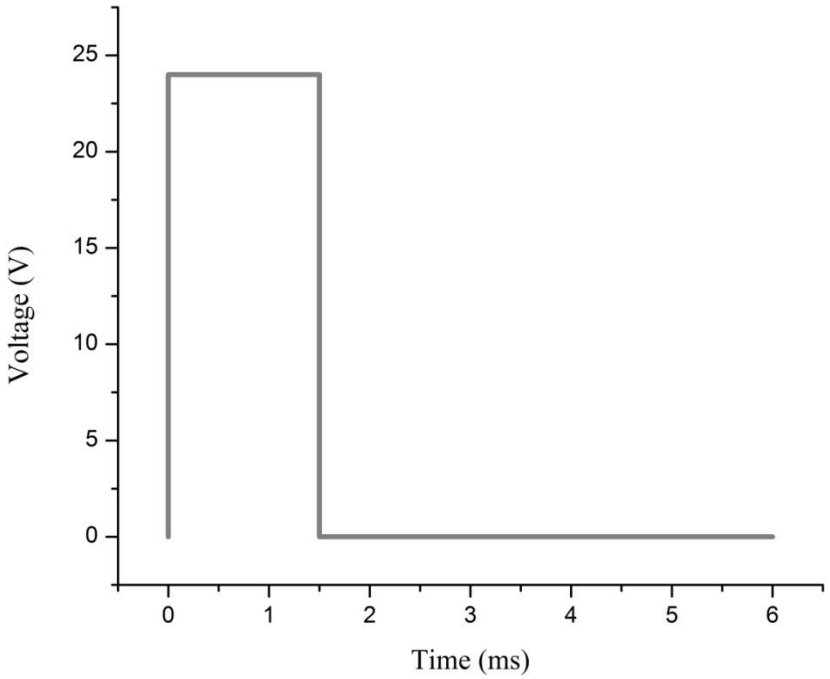

Figure 9 Input voltage Signal for LPM (24V)

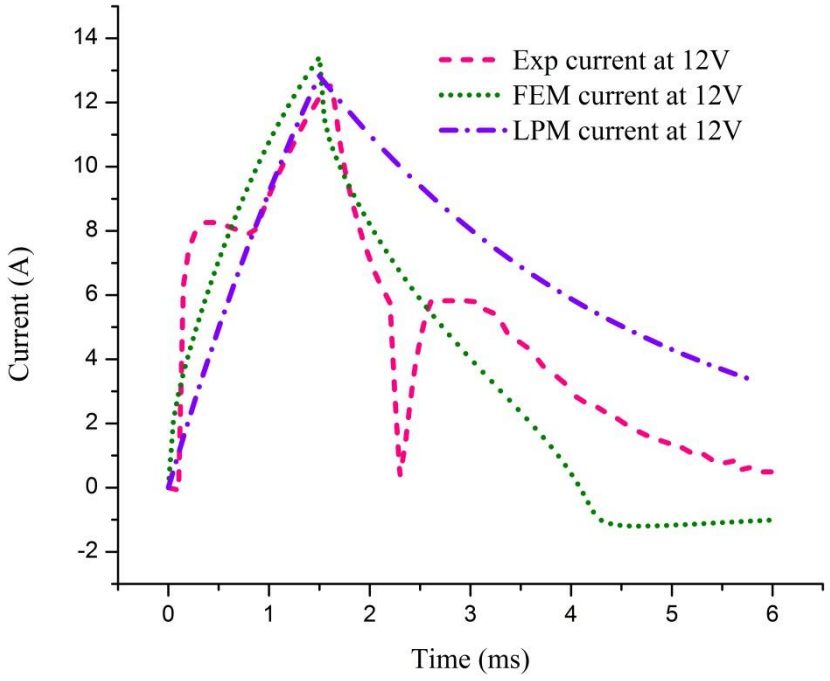

Figure 10 Comparison of current response at 12V and 0.5mm (linear system)

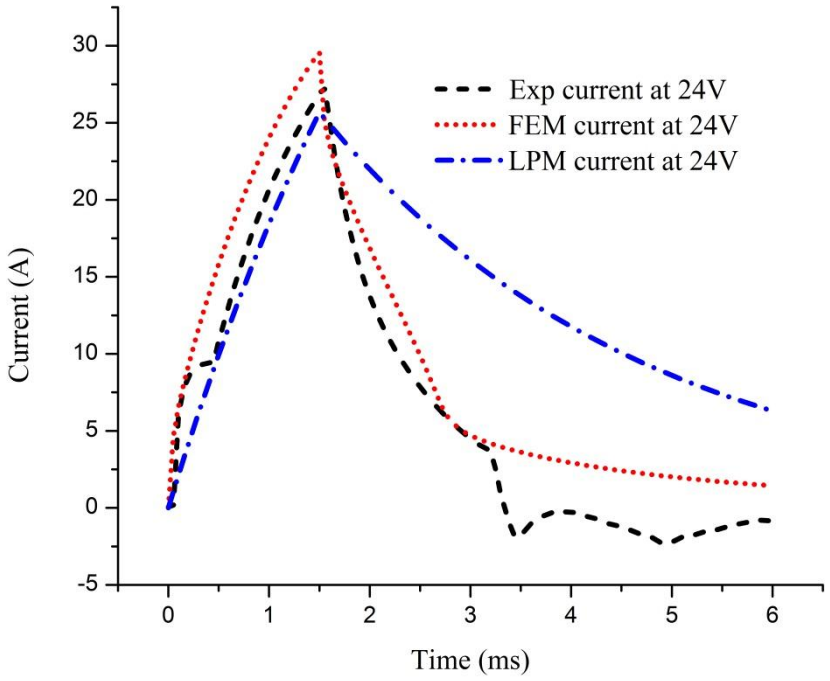

Figure 11 Comparison of current response at 24V and 0.5mm (linear system)

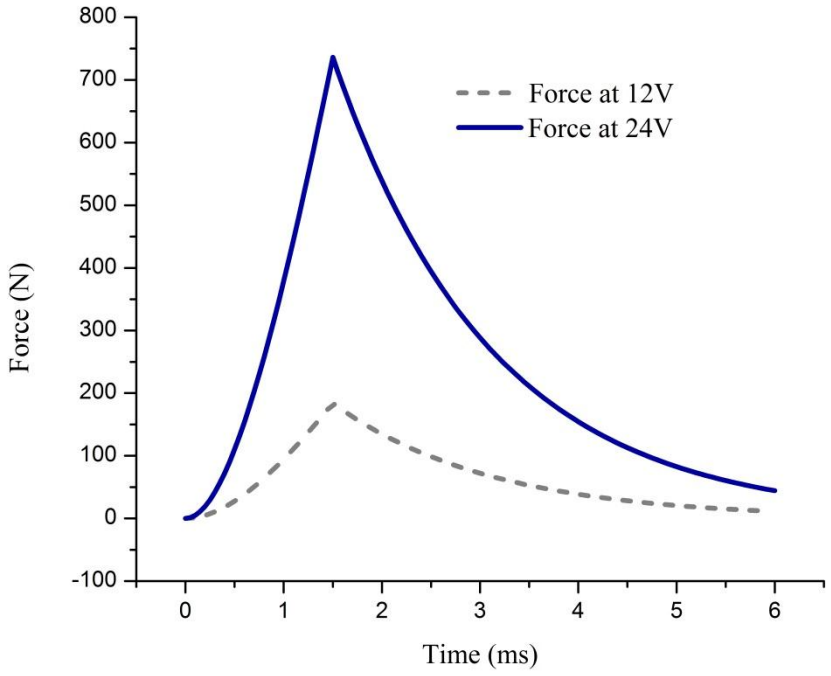

Figure 12 Force Comparison at 0.5mm with 12V and 24V (Linear system)

The force response for LPM using simplified linear system gives peak current of 736N at 0.5mm with 24V time constrained signal. The force peak can be compared with peak force observed for static experimentation with error of 0.8%. The current for static experimentation was restricted to magnitude lower than 10A to avoid overheating issues. The higher current peak for LPM response is due to higher duration of continuous voltage signal as compared to static experimentation. The force peak at 12V is of lower magnitude as compared to 24V peak current.

The LPM current response for nonlinear system shows agreement within 10% error compared with FEM and experimental responses at 12V. The error observed is within 15% compared with FEM and experimental results at 24V. The LPM force response for 24V signal at 0.5mm shows peak of 839N and the peak observed for 12V signal is 193N. The comparison of LPM developed using linear and nonlinear system of equations showed comparable results for current and force peaks. The LPM current responses for nonlinear system are shown in Fig. 13, 14 and force response in Fig. 15.

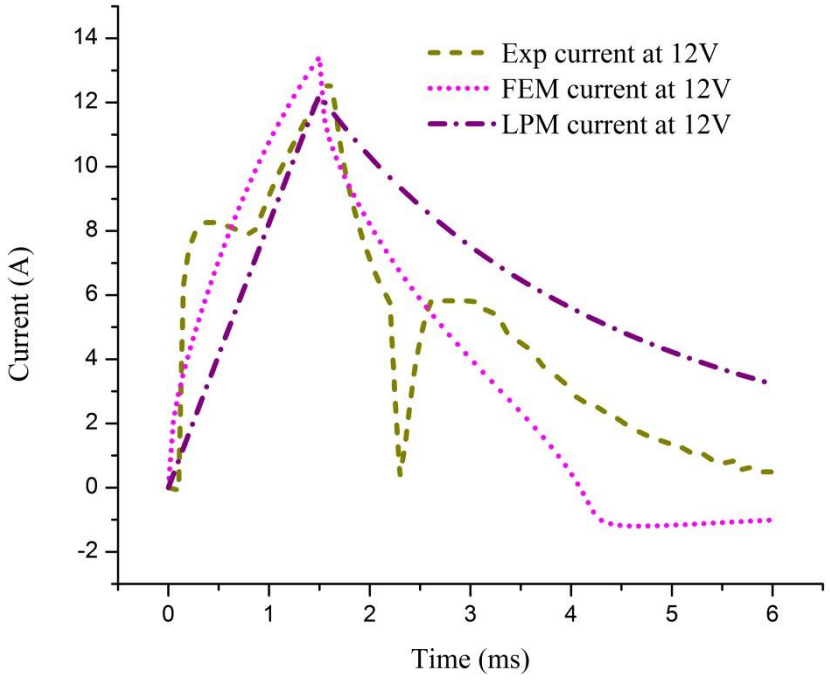

Figure 13 LPM, FEM and experimental current comparison at 0.5mm and 12V (nonlinear system)

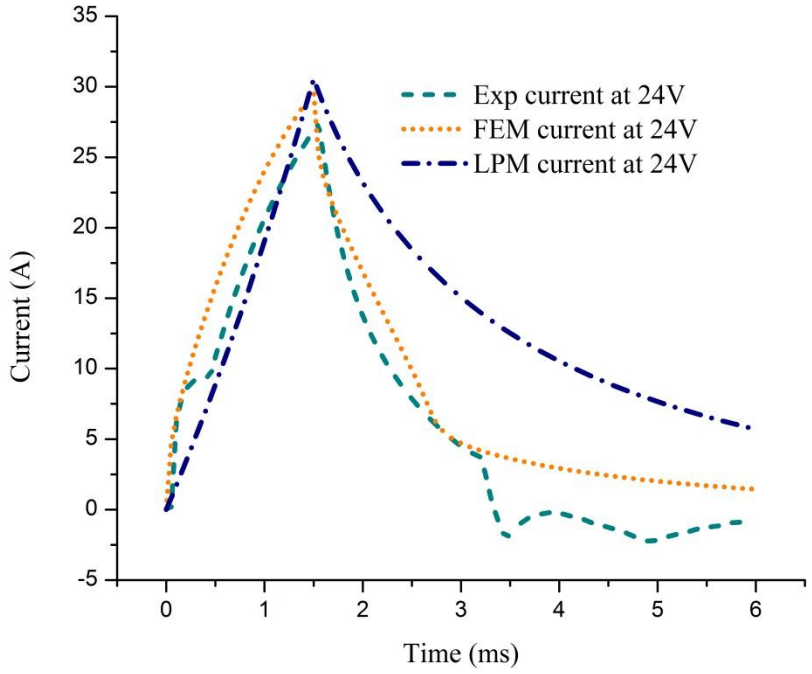

Figure 14 LPM, FEM and experimental current comparison at 0.5mm and 24V (nonlinear system)

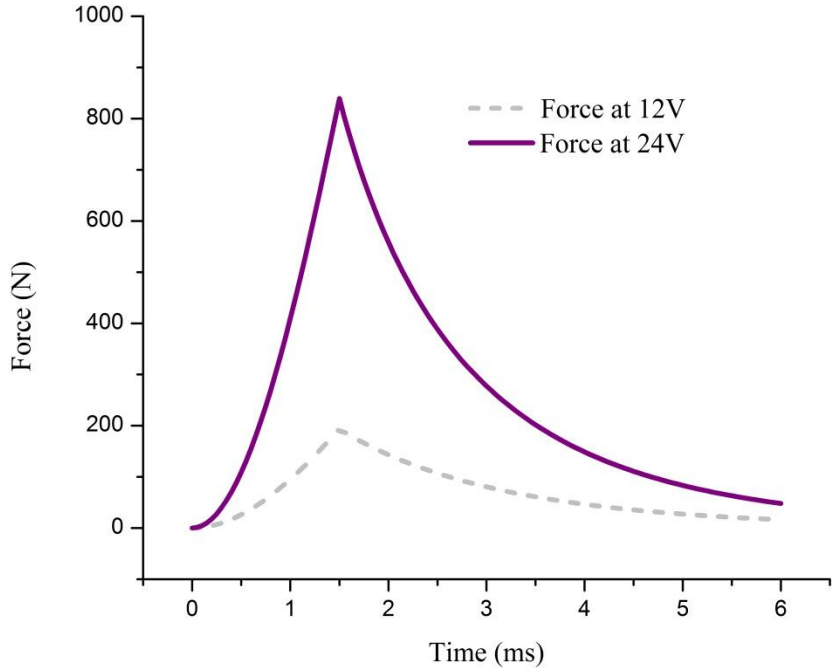

Figure 15 LPM Force comparison at 0.5mm with 12V and 24V (nonlinear system)

5.3 Displacement and velocity responses

The armature displacement is restricted to the armature stroke of 8mm according to the design and fabrication of MHVA. The armature displacement starts from one extreme position to the other extreme position between the restricted stroke length. The initial point is selected to be -4mm for both systems. The displacement and velocity variations for linear system are shown in Fig. 16, 17 and nonlinear system in Fig. 18, 19. The armature reaches the extreme position of 3.73mm and 3.75mm for linear and nonlinear systems with -4mm as starting position. The velocity peak values are1.5m/s for both the systems. Only opener coil is considered for the purpose of modeling. The closer coil behaves in the similar manner to the opener coil and hence it is not modeled in this study.

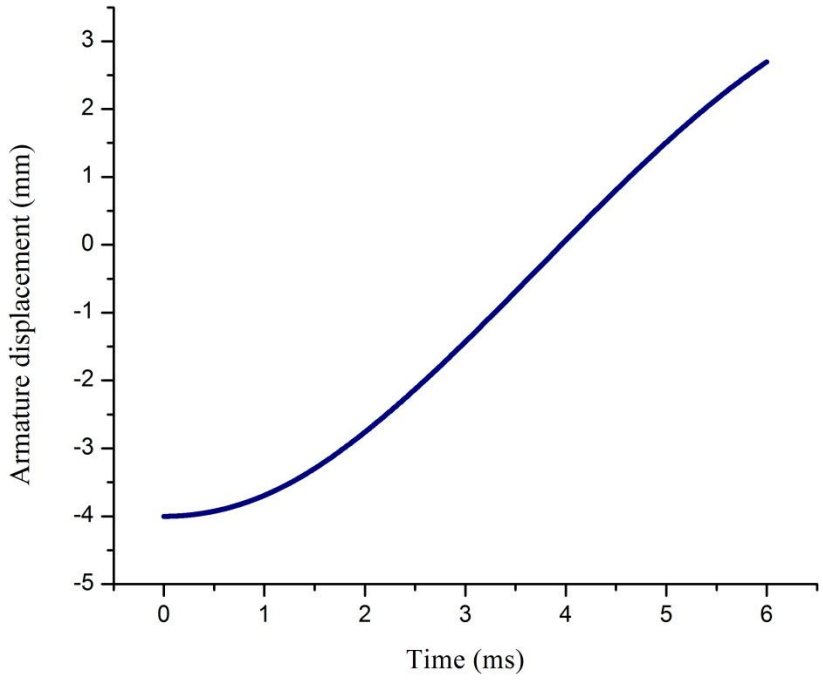

Figure 16 Armature displacement (linear system)

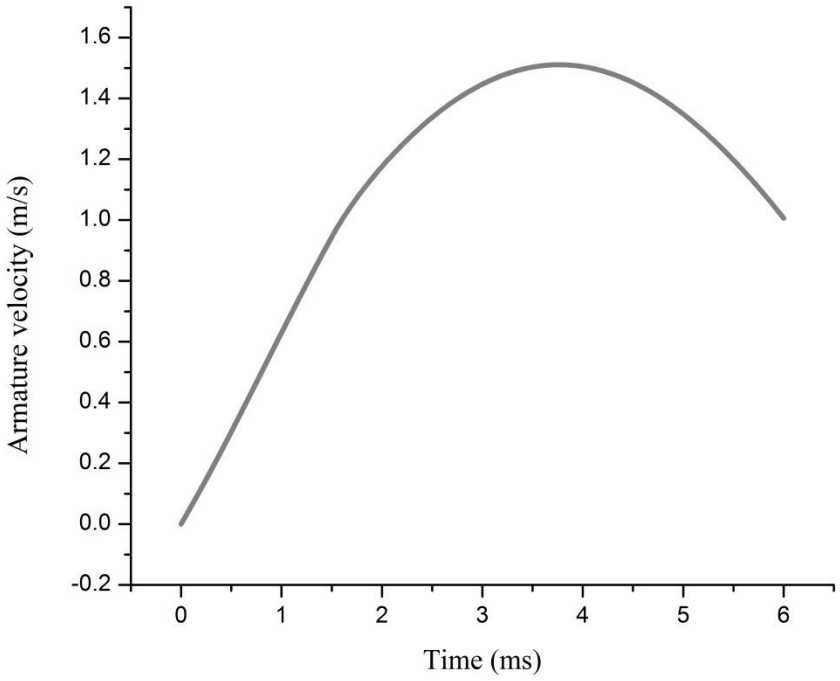

Figure 17 Armature velocity (linear system)

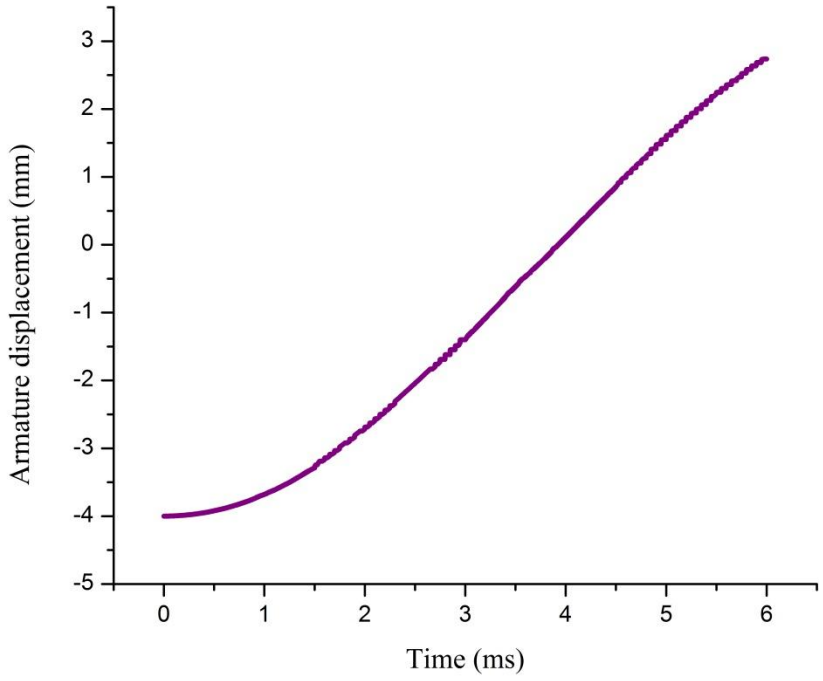

Figure 18 Armature displacement (nonlinear system)

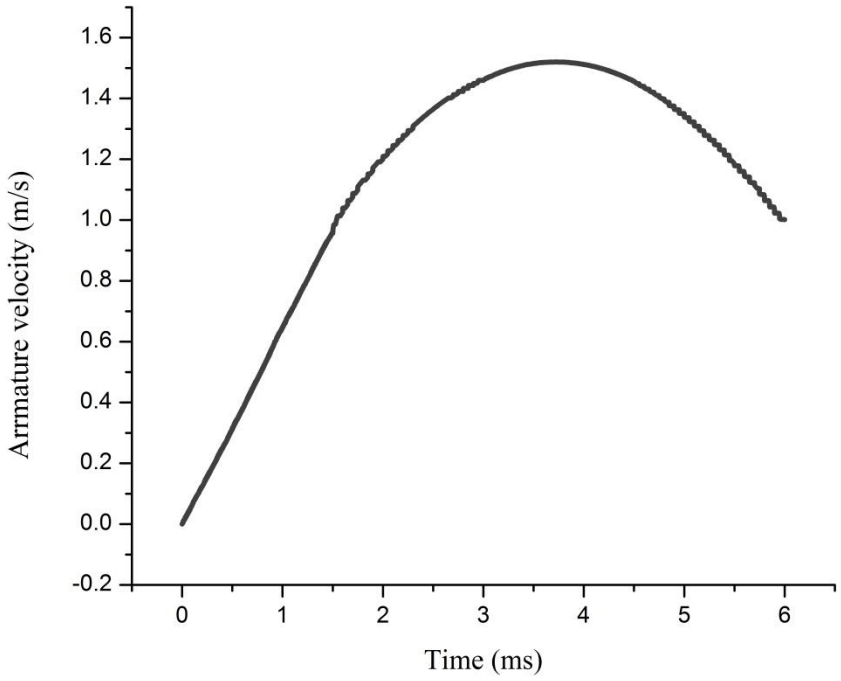

Figure 19 Armature velocity (nonlinear system)

5.5 Summary

The results obtained from experimentation, FEM and LPM are compared in this chapter for both linear and nonlinear systems including the comparative study of coil current, force due to electromagnet and permanent magnet, displacement and velocity of armature of MHVA. The comparison of current show agreement in the overall trend observed for the three different methodologies of experimentation, FEM and LPM.. The overall force behavior shows agreement of results for experimental, FEM and LPM. The force model developed in LPM includes the effect of both the electromagnet and permanent magnets. The displacement for both the cases starts with -4mm position and approaches the other extreme position of 4mm for experimentation and LPM in the fixed 8mm stroke length. The velocity response shows positive and negative peaks of nearly the same magnitude in LPM with negative peaks indicating the change in the direction of motion of armature. The comparative study indicates the agreement of experimental FEM and LPM results validating the LPM developed on the basis of two different systems of mathematical expressions and physical parameters extracted from curve fitting of experimental static force results using S-function in Simulink module of MATLAB.

CHAPTER 6: CONCLUSION AND FUTURE WORK

Automobile engine valve actuation is of primary importance in the fuel efficient engine design and development. Electromechanical valve actuation system is among the important and most studied valve actuation system during the past few years. The utilization of valve actuation systems can replace the conventional camshaft to operate the valves in the internal combustion automobile engines. The electromechanical valve actuation system operates on the input voltage signal generating the coil current and electromagnetic force for the displacement of armature in a confined stroke length of 8mm resulting in the opening and closing of fuel intake and exhaust valves in the automobile engine. A lumped parameter model of MHVA is developed in this thesis based on experimental and FEM results of previous study by J. Aslam *et al* [41] and mathematical expressions for related physical properties using S-function of Simulink module of MATLAB. The LPM developed in this thesis has the advantage of reduction of time and less burden of computation as compared to both the FEM development and real life fabrication and experimentation. The methodology and the outcomes of the thesis are listed below.

1. Physical parameters are identified using the static force data obtained from the experimentation of MHVA performed by previous study. Least square curve fitting technique is performed on the experimental force data to obtain important physical quantities required for mathematical modeling of MHVA system. The curve fitting is performed using Origin data analysis software.
2. The curve fitting performed using Origin is optimized to achieve single best fit parameters for the multi-data set. The global fit of nonlinear curve fit in the Origin is used for curve fitting and shared parameter option is used to obtain optimized and shared parameters which are best fit to the overall data set.
3. After the identification of physical parameters, the mode is developed using a set of mathematical equations representing physical quantities including coil current, permanent and electromagnetic force, armature displacement and velocity. The modeling of MHVA is performed using S-function in Simulink module of MATLAB. Individual subsystems are developed for current, force, displacement and velocity modeling and are integrated to form lumped parameter model (LPM).

4. In the electrical subsystem, the model of current is developed using differential equation representing the behavior of coil current with variation of time, voltage, coil resistance, armature displacement, armature velocity and physical parameters identified by the curve fitting of experimental force data. The input to the subsystem is a step voltage of 12V and 24V magnitude with a step of 1.5ms as the same step time was used in the design and experimentation of MHVA in the previous study for comparison and validation of mathematical model. The subsystem is developed in Simulink window using user defined function known as S-function.
5. In the magnetic subsystem, the force model is developed using a mathematical equation representing the variation of force with coil current which is obtained as an output from the electrical subsystem. The mathematical equation also includes the physical parameters obtained from curve fitting of experimental force data, armature displacement. The effect of permanent magnet force is included in the model in addition to the electromagnetic force. The PM force is assumed to have some value of current as EM force curves have fixed current values during the curve fitting in Origin to include its effect in modeling. The force subsystem is developed using S-function of Simulink.
6. In the mechanical subsystem, the model of armature displacement and velocity is developed using the mathematical expression of forced and damped spring mass system with external force obtained as an output from the magnetic subsystem. The spring constant and viscous damping coefficient are of same magnitude as used in the previous study for comparison and validation of model. The output of the subsystem of the system is integrated to obtain velocity and further integrated to obtain displacement of armature. The displacement and velocity are used as input to the electrical and magnetic subsystem.
7. The comparative study is performed to validate the results of LPM. The results of LPM are compared with both the experimental and FEM results. The overall current behavior shows agreement between results of three different methodologies. The higher the input voltage, the higher the magnitude of current. The force peak values are obtained at the other extreme position of armature opposite to the initial extreme position and the peak values are comparable for the three methodologies. The armature displacement variation is nearly the same with 8mm as the initial extreme position and approximately 0mm as the other extreme position. The velocity peak values are comparable with the LPM showing positive and

negative peaks of approximately same magnitude. The negative velocity values indicate the opposite direction of armature movement. The peak velocity values for both experimental and LPM are observed at the equilibrium position of armature movement and lowest values at both the extreme positions.

8. The comparative study shows close agreement between the results of experimentation, FEM and LPM which indicate the LPM developed in this thesis is valid. The slight differences in the values are observed as the mathematical expressions cannot incorporate all the complexities and nonlinearities associated with the real life experimentation.

6.1 Future work

The design and development of automobile engine valve actuation system to replace conventional camshaft is an important topic in the field of internal combustion engines. Despite of extensive research in this area, the technology of camless valve actuation systems are still not fully commercialized due to non-feasibility in the long term application of actuation system in the automobile engines. The FEM and experimentation of MHVA was performed in the previous study by J. Aslam *et al* [41] and the LPM of MHVA with the same specification used in the FEM and experimentation is developed in this study. Following steps highlight the future work in this area**.**

1. The LPM developed in this study incorporates the material saturation, field solution and can be further enhanced to include the effects of eddy current, flux leakage.
2. The LPM model can be enhanced to include the effects of varying gas pressure disturbances of real engines and pressure cavity must be first included in the experimental test bed for comparison and validation of LPM.
3. The hydraulic lash adjuster can be included in the LPM for more realistic dynamic behavior of model and must also be implemented in the test bed for comparison and validation.
4. The dynamics of bounce of valve actuator can be included for realistic behavior modeling of actuator.
5. Different control strategies for controlling the valve seating dynamics can be designed and developed using the LPM developed in this study. The control implemented on the basis of LPM can be included in the experimental test bed to test the effectiveness of control implantation.

6. The effect of control implemented on the mechanical properties including stress, strain, fatigue, creep and other properties can be tested to validate the effectiveness of various control strategies.
7. The cost effective solution of control implementation can be included to compare different control implantation on the test bed for commercial use in the automobile engines.
8. Alternative valve actuation systems including hydraulic, pneumatic, and piezoelectric and combination of more than one actuation systems can be designed and validated on FEM and experimental test beds. LPM can be developed for the actuation system and control strategy can be implemented on the basis of LPM and tested on experimental test bed.

REFERENCES

[1] F. Bonatesta, G. Altamore, J. Kalsi, and M. Cary, "Fuel economy analysis of part-load variable camshaft timing strategies in two modern small-capacity spark ignition engines," *Applied energy,* vol. 164, pp. 475-491, 2016.

[2] C. Tai and T.-C. Tsao, "Control of an electromechanical actuator for camless engines," in *American Control Conference, 2003. Proceedings of the 2003*, 2003, pp. 3113-3118.

[3] M. M. Schechter and M. B. Levin, "Camless engine," SAE Technical Paper 0148-7191, 1996.

[4] R. R. Henry, "Single-cylinder engine tests of a motor-driven, variable-valve actuator," SAE Technical Paper 0148-7191, 2001.

[5] Z. Sun and D. Cleary, "Dynamics and control of an electro-hydraulic fully flexible valve actuation system," in *American Control Conference, 2003. Proceedings of the 2003*, 2003, pp. 3119-3124.

[6] Z. Sun and T.-W. Kuo, "Transient control of electro-hydraulic fully flexible engine valve actuation system," *IEEE Transactions on Control Systems Technology,* vol. 18, pp. 613-621, 2010.

[7] C. Kaddissi, J.-P. Kenne, and M. Saad, "Indirect adaptive control of an electrohydraulic servo system based on nonlinear backstepping," *IEEE/ASME transactions on mechatronics,* vol. 16, pp. 1171-1177, 2011.

[8] H. Li, Y. Huang, G. Zhu, and Z. Lou, "Linear Parameter-Varying Model of an Electro-Hydraulic Variable Valve Actuator for Internal Combustion Engines," *Journal of Dynamic Systems, Measurement, and Control,* vol. 140, p. 011005, 2018.

[9] P. Wong and K. Mok, "Design and modeling of a novel electromechanical fully variable valve system," SAE Technical Paper 0148-7191, 2008.

[10] H.-H. Liao, M. J. Roelle, and J. C. Gerdes, "Repetitive control of an electro-hydraulic engine valve actuation system," in *American Control Conference, 2008*, 2008, pp. 975-980.

[11] J. Ma, G. G. Zhu, and H. Schock, "A dynamic model of an electropneumatic valve actuator for internal combustion engines," *Journal of dynamic systems, measurement, and control,* vol. 132, p. 021007, 2010.

[12] J. Ma, G. G. Zhu, and H. Schock, "Adaptive control of a pneumatic valve actuator for an internal combustion engine," *IEEE Transactions on Control Systems Technology,* vol. 19, pp. 730-743, 2011.

[13] T. Nguyen, J. Leavitt, F. Jabbari, and J. Bobrow, "Accurate sliding-mode control of pneumatic systems using low-cost solenoid valves," *IEEE/ASME Transactions on mechatronics,* vol. 12, pp. 216-219, 2007.

[14] N. Jalili, J. Wagner, and M. Dadfarnia, "A piezoelectric driven ratchet actuator mechanism with application to automotive engine valves," *Mechatronics,* vol. 13, pp. 933-956, 2003.

[15] B. Haus, H. Aschemann, P. Mercorelli, and N. Werner, "Nonlinear modelling and sliding mode control of a piezo-hydraulic valve system," in *Methods and Models in Automation and Robotics (MMAR), 2016 21st International Conference on*, 2016, pp. 442-447.

[16] R. R. Chladny, C. R. Koch, and A. F. Lynch, "Modeling automotive gas-exchange solenoid valve actuators," *IEEE Transactions on Magnetics,* vol. 41, pp. 1155-1162, 2005.

[17] C. Niţu, B. Grămescu, and S. Niţu, "Application of electromagnetic actuators to a variable distribution system for automobile engines," *Journal of materials processing technology,* vol. 161, pp. 253-257, 2005.

[18] F. Ronchi, C. Rossi, and A. Tilli, "Sensing device for camless engine electromagnetic actuators," in *IECON 02 [Industrial Electronics Society, IEEE 2002 28th Annual Conference of the]*, 2002, pp. 1669-1674.

[19] Y. Qiu, D. J. Perreault, J. G. Kassakian, and T. A. Keim, "A CUSTOM-DESIG ED LIMITED-A GLE ACTUATOR FOR A ELECTROMECHA ICAL E GI E VALVE DRIVE PART II: FABRICATIO AD EVALUATIO."

[20] K. Nagaya, H. Kobayashi, and K. Koike, "Valve timing and valve lift control mechanism for engines," *Mechatronics,* vol. 16, pp. 121-129, 2006.

[21] S. Khan, M. Cai, K. Grattan, K. Kajan, M. Honeywood, and S. Mills, "Design and investigation of high-speed, large-force and longlifetime electromagnetic actuators by finite element modelling," in *Journal of Physics: Conference Series*, 2005, p. 300.

[22] L. Liu and S. Chang, "Improvement of valve seating performance of engine's electromagnetic valvetrain," *Mechatronics,* vol. 21, pp. 1234-1238, 2011.

[23] A. di Gaeta, L. Glielmo, V. Giglio, and G. Police, "Modeling of an Electromechanical Engine Valve Actuator Based on a Hybrid Analytical--FEM Approach," *IEEE/ASME Transactions on Mechatronics,* vol. 13, pp. 625-637, 2008.

[24] Y.-P. Yang, J.-J. Liu, D.-H. Ye, Y.-R. Chen, and P.-H. Lu, "Multiobjective optimal design and soft landing control of an electromagnetic valve actuator for a camless engine," *IEEE/ASME Transactions on Mechatronics,* vol. 18, pp. 963-972, 2013.

[25] S. H. Lee, H. C. Yi, K. Han, and J. H. Kim, "Genetic algorithm-based design optimization of electromagnetic valve actuators in combustion engines," *Energies,* vol. 8, pp. 13222-13230, 2015.

[26] P. Mercorelli, "A motion-sensorless control for intake valves in combustion engines," *IEEE Transactions on Industrial Electronics,* vol. 64, pp. 3402-3412, 2017.

[27] A. Fabbrini, A. Garulli, and P. Mercorelli, "A trajectory generation algorithm for optimal consumption in electromagnetic actuators," *IEEE Transactions on Control Systems Technology,* vol. 20, pp. 1025-1032, 2012.

[28] J. Tsai, C. R. Koch, and M. Saif, "Cycle adaptive feedforward approach controllers for an electromagnetic valve actuator," *IEEE Transactions on Control Systems Technology,* vol. 20, pp. 738-746, 2012.

[29] S. K. Chung, C. R. Koch, and A. F. Lynch, "Flatness-based feedback control of an automotive solenoid valve," *IEEE Transactions on Control Systems Technology,* vol. 15, pp. 394-401, 2007.

[30] C. R. Koch, A. F. Lynch, and R. R. Chladny, "Modeling and control of solenoid valves for internal combustion engines," *IFAC Proceedings Volumes,* vol. 35, pp. 197-202, 2002.

[31] E. Melgoza and D. Rodger, "Comparison of table models of electromagnetic actuators," *IEEE transactions on magnetics,* vol. 38, pp. 953-956, 2002.

[32] D. Cope, A. Wright, C. J. Corcoran, K. Pasch, and D. Fischer, "Fully flexible electromagnetic valve actuator: design, modeling, and measurements," SAE Technical Paper 0148-7191, 2008.

[33] Y. Shiao and L. V. Dat, "Actuator control for a new hybrid electromagnetic valvetrain in spark ignition engines," *Proceedings of the Institution of Mechanical Engineers, Part D: Journal of Automobile Engineering,* vol. 227, pp. 789-799, 2013.

[34] J. Kim and D. K. Lieu, "Designs for a new, quick-response, latching electromagnetic valve," in *Electric Machines and Drives, 2005 IEEE International Conference on*, 2005, pp. 1773-1779.

[35] J. S. Brader, N. R. Trevett, and D. N. Rocheleau, "Advances in Actuation Systems to Improve Vehicle Performance and Safety," in *ASME 2003 International Mechanical Engineering Congress and Exposition*, 2003, pp. 105-111.

[36] P. Mercorelli, "A switching kalman filter for sensorless control of a hybrid hydraulic piezo actuator using mpc for camless internal combustion engines," in *Control Applications (CCA), 2012 IEEE International Conference on*, 2012, pp. 980-985.

[37] P. Mercorelli, "An adaptive and optimized switching observer for sensorless control of an electromagnetic valve actuator in camless internal combustion engines," *Asian Journal of Control,* vol. 16, pp. 959-973, 2014.
[38] P. Mercorelli and N. Werner, "A hybrid actuator modelling and hysteresis effect identification in camless internal combustion engines control," *International Journal of Modelling, Identification and Control 5,* vol. 21, pp. 253-263, 2014.
[39] J.-J. Liu, Y.-P. Yang, and J.-H. Xu, "Electromechanical valve actuator with hybrid MMF for camless engine," *IFAC Proceedings Volumes,* vol. 41, pp. 10698-10703, 2008.
[40] P. Mercorelli and N. Werner, "Integrating a piezoelectric actuator with mechanical and hydraulic devices to control camless engines," *Mechanical Systems and Signal Processing,* vol. 78, pp. 55-70, 2016.
[41] J. Aslam, X.-h. Li, and F. K. Janjua, "Design of a hybrid magnetomotive force electromechanical valve actuator," *Frontiers of Information Technology & Electronic Engineering,* vol. 18, pp. 1635-1643, 2017.

APPENDIX

The individual s-function subsystems developed in the Simulink with the step input voltage signal, the output of the subsystems and the feedback of some outputs to the input ports is represented in the snapshot shown below taken from the Simulink window of MATLAB. Each s-function subsystem has an associated m-file for definition of mathematical function and initial conditions with values of physical parameters obtained from the experimental and FEM results of previous study. The snapshot of both the LPMs developed in Simulink window of MATLAB is shown in Fig. 13.

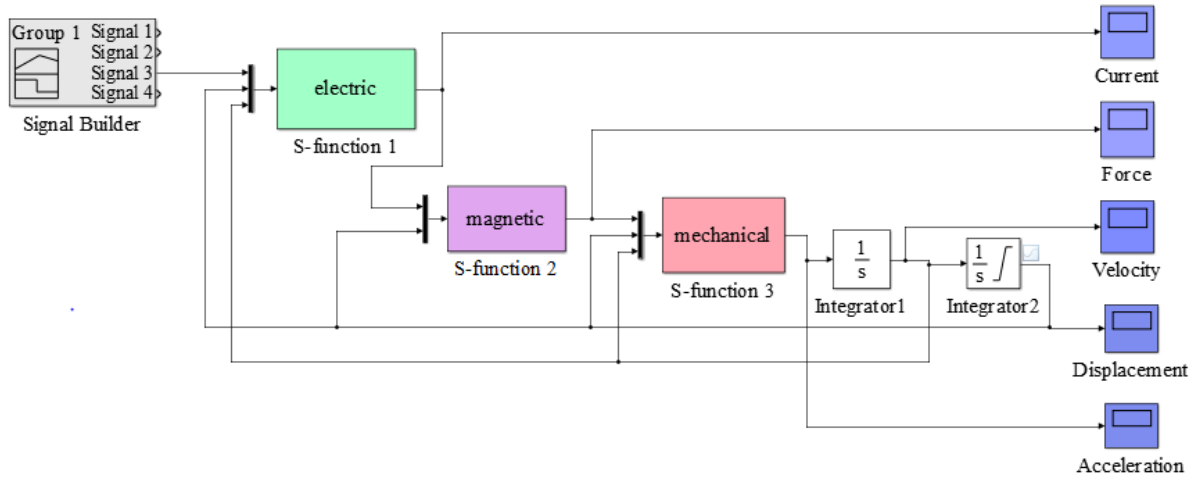

Figure 20 LPM snapshot from Simulink window